Giant planet formation around HR8799

Dan Wallsby

Lund Observatory
Lund University

2017-EXA111

Degree project of 60 higher education credits (for a degree of Master)
May 2017

Supervisor: Bertram Bitsch

Lund Observatory
Box 43
SE-221 00 Lund
Sweden

Abstract

In the thriving field of exoplanet research new discoveries are made all the time, and while most of the observed systems can be explained with classical planet formation models - some are much harder to explain. When stars form they are often surrounded by the remaining material of the nebulae they formed from. Some of this remaining material forms into a protoplanetary disk around the protostars due to the conservation of angular momentum and the intrinsic movement of the gas, in this protoplanetary disk planets can form. Planet formation depend strongly on the environment in which they form, so the properties and evolution of protoplanetary disks is an important part of understanding planet formation. In the case of stars that are more massive then the Sun this field is largely unexplored.

In this project we look closer to one of these systems, HR8799. That, as will be shown, is not obvious how it formed and evolved. We explore the protoplanetary disk and its evolution around a young 1.47 solar mass star using a temperature structure as a function of radius and hydrodynamic simulations. This disk structure will serve as an environment for planet formation to recreate HR8799, which is an observed exoplanet system with four super jovian planets (5+ Jupiter mass) on wide orbits(14.5, 24, 38 and 68AU). To grow and evolve the modeled planets we use a N-body code in a parameterized space that represents the protoplanetary disk, in which we place planet seeds and let them grow by pebble and gas accretion while including migration, interactions with the protoplanetary disk and dynamics between the planets.

Starting the simulation with four planets, we define a stable system as one where no collisions or ejections of planets occur. We find that the survival rate of systems is below 10% and there are multiple parameters that influence the survival rate. Our search focused on the viscosity parameter α as it greatly affects the disk structure, that in turn affects the planets growth and migration. We also varied the disk age and the pebble metallicity. We do not find an exact match for HR8799 in our survivors, but we do find stable systems with four giant planets, over three Jupiter masses ($3M_{Jup}$) on wide orbits, where the outer planet is on >50 AU orbit. In this thesis I will show that it is possible to grow and evolve stable systems with giant planets on wide orbits via pebble accretion as main core growth mechanism.

Populärvetenskaplig beskrivning

I det blomstrande forskningsfältet om planeter och exoplaneter, det vill säga planeter utanför vårat eget Solsystem hittar vi konstant nya planeter och system som alla ger oss pusselbitar till att förstå hur planeter formas och utvecklas. Så för att förstå de observationer vi gör och bedöma hur sannolikt det är att det kan finnas liv på en planet, måste vi förstå alla olika typer av system och hur de formas.

I det är projektet är målet att återskapa ett observerat exoplanetsystem, HR8799. Det är ett ovanligt system med fyra väldigt massiva planeter på vida omloppsbanor runt sin stjärna. Kombinationen av dessa är ovanligt då massiva planeter både har en tendens att göra systemet instabilt, som leder till att planeter kolliderar eller blir utkastade. Eller att de massiva planeterna migrerar väldigt nära sin stjärna och blir en så kallad ”het Jupiter”, en klass av planeter som vi inte har i Solsystemet med är vanlig kring andra stjärnor.

Det första steget i projektet är att först och bygga upp en modell av en protoplanetär disk runt stjärnan, som är resterna från nebulosan som stjärnan skapades ifrån. Genom bevaring av rörelsemängdsmoment och gasens rörelse plattas den ner till en roterande skiva runt stjärnan. I denna gasrika disk bildas planeter, asteroider och allt annat som kretsar kring en stjärna efter gasen har försvunnit.

Efter en diskmodell är uppbyggd kommer vi att plantera planetesimaler i storleksordning av några procent av en jordmassa och låta dem växa genom att krocka med och dra åt sig material från disken samtidigt som disken utvecklas och planeterna påverkar varandra via gravitation.

Vi finner att det är få (8%) av systemen som överlever, men några gör det. Även om vi inte finner ett system exakt som HR8799 så hittar vi stabila system med fyra massiva planeter på vida omloppsbanor som är jämförbara med HR8799. Resultaten vi har berättar för oss att det är svårt, men möjligt att bygga multipla, massiva planeter på vida omloppsbanor med en model där man först bygger upp en planetkärna och sen drar till sig en massiv gas atmosfär.

Contents

List of Figures

Chapter 1

Introduction

One of the motivations for exoplanet research is to find habitable planets, but these terrestrial planets are just a small part of the many types of planets that are discovered. To understand the big picture on how planetary systems form and evolve we must understand the formation process for all types of planets. In this project we focus on one observed exoplanet system named HR8799 with four massive planets on wide orbits, discussed in section 1.1.

Some claim that it is likely that HR8799 formed via a gravitational instability in the protoplanetary disk, as this planet formation model tend to form massive planets on wide orbits. But there are strong arguments against this claim, as discussed in section 1.3.1.

In this project we use a core accretion model that first builds the core of the planet and then accrets the gaseous envelope. To the classical planetesimal accretion model (discussed in section 1.3.2) we add pebble accretion as explained in section 1.3.3. So a big part of this project is to test the limits of pebble accretion for giant planet formation - can the model grow the cores fast enough on wide orbits where the density is low? or will the growth rate vary too much as a function of the distance from the star? and how will the dynamics between the growing planets affect the system? These are some of the main questions we aim to answer.

In addition to the previous main questions we will also probe and help constrain some parameters (α and pebble metallicity $Z = \Sigma_p/\Sigma_g$) in protoplanetary disks for giant planet formation.

Since we want to build the planet cores by pebble accretion we have to take some restrictions into account; the disk must remain stable, meaning I have to make sure that the protoplanetary disk is not too massive, as this is one of the criteria for an unstable disk (Toomre criteria: Toomre 1964). The second criteria is, that the cooling time in the disk must be fast enough, because for the gas to contract it must cool fast enough (Gammie critera: Gammie 2001). There criteria are discussed in section 2.3.

1.1 HR8799

HR8799 is not a system that represents the norm in any sense, but is rather a rare jewel that puzzles us with questions about how it formed and if it can be explained with existing models and methods. What makes HR8799 special is the combination of two things; very massive planets that are at very large orbital distances. The previous combination of is an unlikely outcome of the classical planet formation models (that are discussed in section 1.3.1 and 1.3.2). The star that illuminates the HR8799 system is classed as a kA5 hF0 mA5 V star. This rather indecisive classification is due to the fact that the stars temperature and luminosity matches that of a F0 V star, but the Ca II absorption lines matches those of a A5 V star. The star is 1.47$M_{\odot}$ with a surface temperature of 7340K, which makes it nearly 5 times more luminous then the Sun. The metallicity of the star is [Fe/H]=-0.47, this might seem low but for planet formation we must look closer into other elements then only iron, as we care about what mass we have in solids and ices to build planet cores from. So I used the four (C, O, S and Fe) major elements that the literature provided abundances for in HR8799. Then what I wanted to know is what percent of the mass do these make up and how do HR8799 compare to the Sun in that case, giving us an estimate of the solid to gas ratio. The solar mass fractions are from Chainsson & McMillan (1999) and the measurements for HR8799 are from Gray & Kaye (1999), Sadakane (2006) and Moya et al. (2010). Taking all four of these into account the abundance in solids of [Z/H]=0.027, telling us that even though HR8799 is iron poor with respect to the Sun - it is not that low in solids that can form planets as it might seem, this is explained in appendix A.
The first three planets in the system (HR8799bcd) where detected by direct imaging in 2008 (Marois et al. 2008), and the fourth planet was detected two years later (Marois et al. 2010) also with direct imaging. In figure 1.1 we see the detection image of HR8799e, the fourth planet, also including the previous detected b,c and d planets.
Direct imaging means that we see the planet directly, either from the reflected light from the host star in visual wavelengths - this is hard as the host star tend to outshine the planets - we can observe the planets own emitted light in infrared. The latter is possible for either young systems where the planets still maintain some of the heat from the formation process, as the planet needs to be hot to emit bright enough light for it to be detectable. The more time passes the fainter the planet becomes, so the older the system is the further away from the host star the planet needs to be, to be detectable. The four planets in HR8799 were all detected in infrared. Other methods to detect exoplanets rely on an indirect approach, meaning they observe some change in the host star and infer the presence of a planet, but for us humans seeing is believing, so there is something special about seeing the planets directly.
"There's three ways we're going to know if there's other life:
The first is by searching the skies for artificial radio signals. The second is hunting for microbial life within the solar system, in places like Mars or the icy moons of Jupiter and Saturn. And the third method is direct imaging."-Elisa Quintana, a Kepler research scientist with the SETI Institute and the NASA Ames Research Center. There is no substitute to actually seeing a faraway planet with your own eyes.

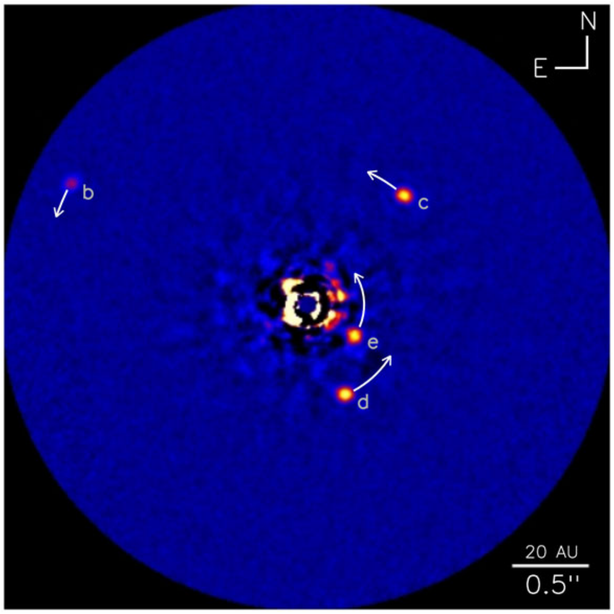

Figure 1.1: Direct imaging of the HR8799 system at the point when HR8799e was discovered (Marois et al. 2010).

HR8799 Facts:

- $M = 1.47 \pm 0.3\mathrm{M}_{\odot}$
- $R = 1.34 \pm 0.05\mathrm{R}_{\odot}$
- $L = 4.92 \pm 0.41\mathrm{L}_{\odot}$
- $T_{eff} = 7340 \pm 75\mathrm{K}$
- 39±1pc away (Pegasus)
- Age=$30^{+20}_{-10}10^6$ years
- Abundance [Z/H]=0.0269±0.0002 Based on C, O, S and Fe abundances.
- HR8799bcde masses $M = 5^{+2}_{-1}, 7^{+3}_{-2}, 7^{+3}_{-2}, 7^{+3}_{-2}M_{Jup}$
- HR8799bcde orbital distance $a = 68 \pm 0, 38 \pm 0, 24 \pm 0, 14.5 \pm 0.5\mathrm{AU}$

1.2 Planetesimals and protoplanets

In this work we are starting our simulations with protoplanets that have already reached the threshold where the protoplanets hill radius (the radius around the object where its gravitational influence dominated over the tidal force from the star) extends beyond the gravitational cross-section (the cross-section around the object where an incoming object will collide with it even if they where not on an crossing path, due to gravitational attraction). This means that the protoplanet can accrete pebbles from the whole hill radius, hence grow faster. This threshold is called the pebble transition mass and given by Lambrechts & Johansen (2014)

$$M_t = \left(\frac{1}{3}\right)^{1/2} \frac{\Omega_k^2}{G} \eta^3 r^3, \tag{1.1}$$

where G is the gravitational constant, r is the distance from the star, Ω_k the Keplerian orbit frequency and η is the difference between gas and Keplerian orbit velocity due to the local pressure gradient, given by,

$$\eta = -\frac{1}{2}\left(\frac{H}{r}\right)^2 \frac{\delta ln(P)}{\delta ln(r)}, \tag{1.2}$$

where P is the pressure and H is the scale height,

$$H = \frac{c_s}{\Omega_k}, \tag{1.3}$$

where c_s is the sound speed, and

$$\Omega_k = \left(\frac{GM_*}{r^3}\right)^{1/2}, \tag{1.4}$$

where M_* is the mass of the star in solar masses. As the equations show the pebble transition mass is a function of the radius, meaning that the protoplanets will have different initial mass to ensure growth. The transition mass is on the order of a few percent of an Earth mass. This is still small, to small to be even close to the core of a giant planet that range between 10-50 Earth masses. But still quite a bit larger than the formation size of planetesimals formed via the streaming instability (Johansen et al. 2015), that range from $10^{-6} - 10^{-4}$Earth masses (M_E). But as we see the planets there today (about 129 years ago to be exact as that is the time it takes for the light from HR8799 to reach us) they obviously must have formed somehow. Working with a core accretion scenario I am working under the assumption that some of these planetesimals grew from mutual collisions to form the protoplanet seed where pebble accretion is efficient.

1.3 Giant planet formation

Generally speaking there are two different models for planet formation; Core Accretion and Gravitational instability. The major difference being if you grow a planet core from the inside out by accreting material (Core accretion) or if there is a larger instability in the protoplanetary disk that cause a lot of material to fall together very fast (Gravitational instability). Both of these models are feasible for forming planets, so there is no ”right” way. These mechanisms act under different criteria though.

In this project we want to form very massive planets on wide orbits. Therefore we take a closer look on these models and how they work with this in mind in 1.3.1 and 1.3.2.

When forming gas giants we also have a time constraint from observations. To accrete a gaseous envelope there must be gas around to accrete.

We can often constrain many events from observations, protoplanetary disks are no exception. As just mentioned the case of protoplanetary disk, observations can help us constrain their lifetime. From a star we expect nearly a black body spectrum, an excess emission in the near infrared can then act as a probe for a surrounding gas disk. So we can use these observations to constrain the lifetime of the gas disks by observing stellar clusters of different ages and comparing what fraction of the observed stars have an excess emission in the infrared. Which directly gives the same constraints on the formation time for gas giants as they must form while there is gas left in the disk. These observations help us constrain the lifetime of protoplanetary disks to 1-10Myr (Haisch et al. 2001), (Mamajek 2009) as shown in figure 1.2. This means that we must form the gas giants before this time limit, in this project a disk lifetime of 5Myr has been used.

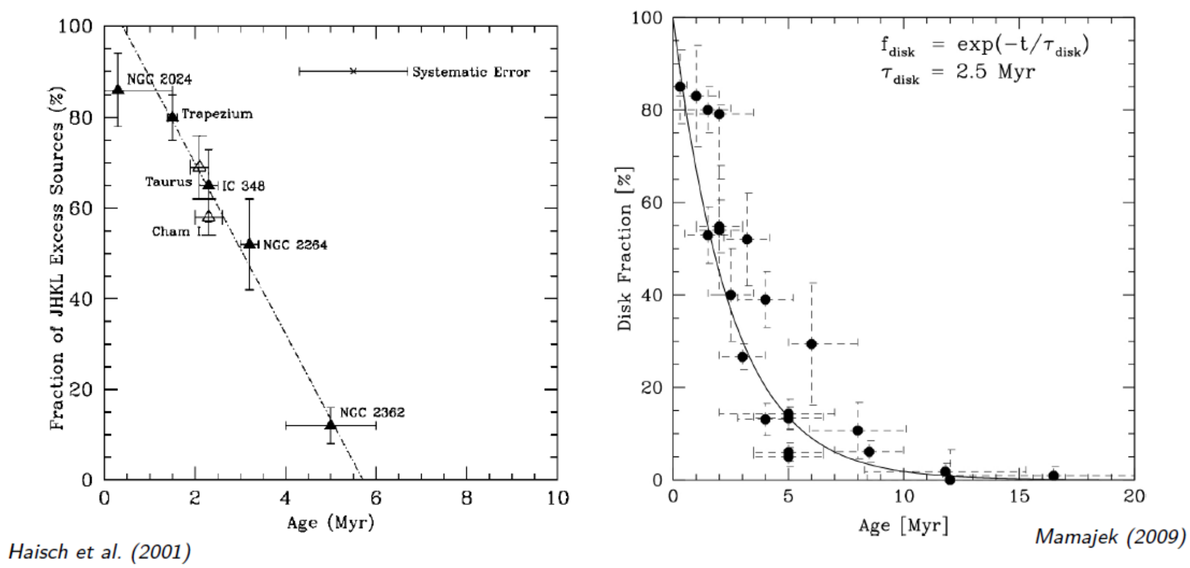

Figure 1.2: Left: Showing the fraction of observed clusters in the JHKL band that show excess disk emission as a function of cluster age (Haisch et al. 2001).
Right: Age of stellar sample vs. fraction of stars with protoplanetary disks either through H-alpha emission or infrared excess diagnostics. As excess emission in the near infrared is a probe for a surrounding gas disk we can use this to constrain the lifetime of the gas disks (Mamajek 2009).

1.3.1 Gravitational instability

The Gravitational instability is a model that looks at a very massive protoplanetary disk and how it can undergo instabilities to form large planets very fast by gravitational collapse, as illustrated in figure 1.3. From these simulations we see that most planets are formed in the outer part of the disk, this is not surprising as that is where most of the mass is. The advantage with this method is that you form massive planets and far away from the host star. The problem is migration and timescales, if the planets form too fast they will have plenty of time to migrate through the protoplanetary disk and will not end up in the outer part where they originally formed. Using hydrodynamic simulations (Baruteau et al. 2011) if a planet formed at 100AU and has a mass of Saturn (M_{Saturn}) the timescale for it to migrate inside 50AU is 3×10^4 years, and for $5M_{Jup}$ it will migrate inside 20AU in 8×10^3 years. As these timescales are very short in respect to the lifetime of the protoplanetary disk, and shorter the higher mass planets are formed, it is highly unlikely that the planets in HR8799 formed this way as they would not end up in the outer part where we observe them. Planetary migration issues are discussed in more detail in section 1.4.

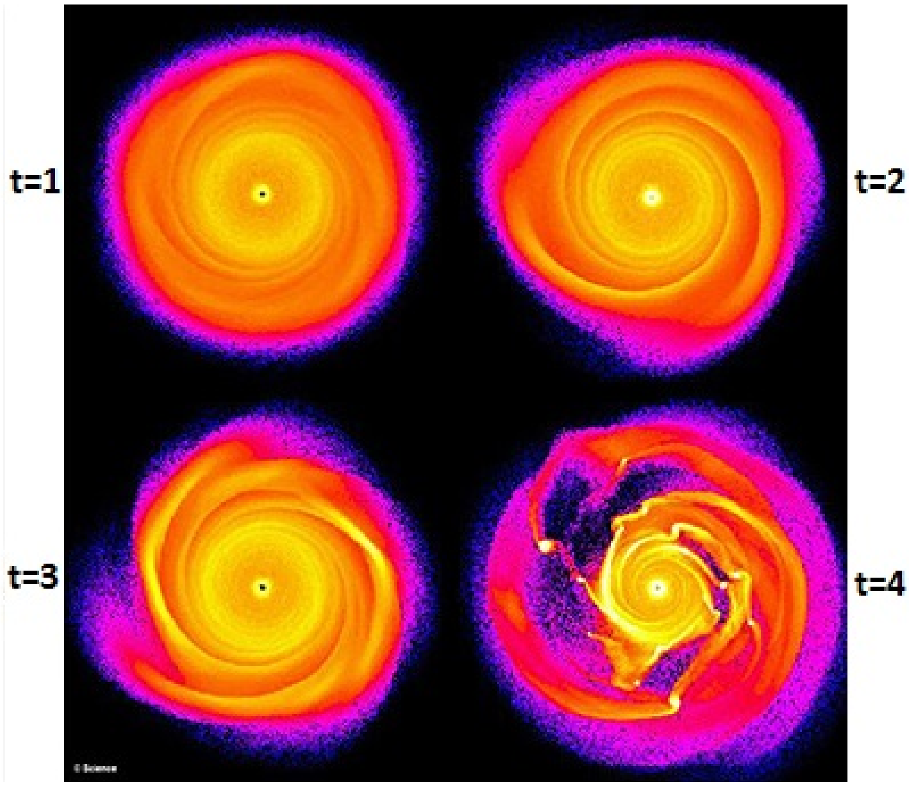

Figure 1.3: Illustration of a massive protoplanetary disk undergoing gravitational collapse into smaller gravitational bound objects, resulting in large planets in the outer part of the disk where most of the mass is. Where t is in arbitrary code units, noted on the plot to indicate that the disk evolves in time. (Simulations numériques de Frédéric Masset (CEA))

1.3.2 Core Accretion model

In the classical Core Accretion model dust grow by collisional sticking until it gets large enough to decouple from the gas and form over-densities that can collapse and form planetesimals, for example via the streaming instability (mentioned in the previous section) (Yang et al. 2015). These planetesimals can then grow by collisions and form the core of future planets.

This process sounds simple enough, but has many hardships to overcome, along with some downsides. As mentioned before, we already assume that planetesimals have formed, so any obstacles up to that point will not be discussed in this thesis. The main obstacle for the planetesimals to grow is time. In astronomy many events occur on very long timescales, ranging from thousands up to billions of years. But as discussed in section 1.3 we have a time limit to form gas giants. The growth of planetesimal by collisions with other planetesimals is very slow, due to the low collision frequency. This problem is even larger the further out in the disk we look, as the density drop with increasing radius. This makes it hard to form the protoplanets we need as initial conditions for this project, so what is missing? Section 1.3.3 will explore the addition to the core accretion model needed to potentially solve this problem.

1.3.3 Pebble accretion

In section 1.3.2 we discussed about the classical way of planetesimal growth by collisions with other planetesimals. But what if, they also grow by accreting pebbles that are observed in large abundances in protoplanetary disks (ALMA Partnership et al. 2015). A pebble is a millimeter to centimeter sized dust aggregate that formed by collisional sticking of micrometer sized dust particles. It is not hard to understand how any massive object would accrete pebbles from the gravitational cross section, illustrated in figure 1.4.

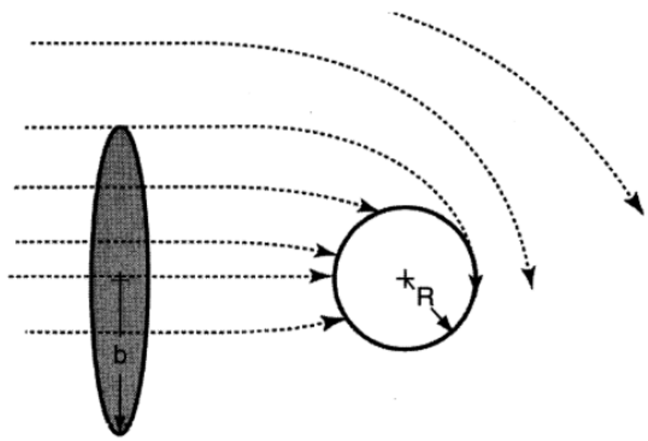

Figure 1.4: Illustration of the gravitational cross section b, in which an incoming object will collide with the planet seed with a radius R.

But here is the big idea, protoplanets can grow by accreting pebbles in their whole hill radii! This radii is much larger then the gravitational cross section, hence a lot more pebbles can be accreted (Lambrechts & Johansen 2012). This works because of the presence of gas in the disk. There is a radial pressure gradient in the protoplanetary disk, as the gas is hotter and denser in the inner region, in effect this results in a inward pressure force onto the gas, causing it on a closer orbit, and to orbit in sub Keplerian velocity. This means that small objects that have not fully decoupled from the gas - such as pebbles, will try to orbit with a Keplerian velocity, this cause the pebbles to feel a headwind from the gas and lose angular momentum, making them drift towards the star. In the big picture this means that pebbles will drift towards the star through the whole disk, resulting in a pebble flux. In the local picture around a protoplanet this means that if a pebble comes within the hill radii it will spiral in to the protoplanet instead of getting scattered like a planetesimal would. Meaning that we can accrete pebbles but not planetesimals from the whole hill radii, as illustrated in figure 1.5. The problem we wanted to solve was that of growth rate, and the growth by pebbles dwarfs that of planetesimals, by a factor close to a thousand (Lambrechts & Johansen 2012), greatly helping the growth of the planet cores.

The gravitational cross section b and hill radii r_{hill} are given by the following equations under the assumption that m≪M where m is the planet mass and M the mass of the star,

$$b^2 = R^2 \left(1 + \frac{v_{esc}^2}{v_\infty^2}\right), \tag{1.5}$$

where R is the radii of the planet, v_{esc} the escape speed and v_∞ the velocity at infinity of the incoming object.

$$r_{hill} = a(1-e)\left(\frac{m}{GM}\right)^{1/3}, \tag{1.6}$$

where a is the semi major axis, e the eccentricity, m the mass of the object we want to know the hill radii of (in this case the planet seeds) and M the mass of the object it is orbiting(in this case the star).

The core accretion rate in 2D is given by Lambrechts & Johansen (2014),

$$\dot{M}_{c,2D} = 2\left(\frac{\tau_f}{0.1}\right)^{2/3} r_{hill} v_{hill} \Sigma_{pebb}, \tag{1.7}$$

where $v_{hill} = \Omega_k r_{hill}$ is the hill velocity, Σ_{pebb} is the pebble surface density and τ_f is the stokes number, given by,

$$\tau_f = \frac{a\rho_{solid}}{H_g \rho_{gas}}, \tag{1.8}$$

Where a is the particle radius, H_g the gas scale height and ρ_{solid} and ρ_{gas} is the solid and gas density respectively. The pebblesurface density is given by,

$$\Sigma_{pebb} = \left(\frac{2\dot{M}_{pebb}\Sigma_g}{\sqrt{3}\pi\epsilon_p r_p v_k}\right)^{1/2}, \tag{1.9}$$

where Σ_g id the gas surface density, r_p the orbital distance at the planets position and v_k is the Keplerian orbit velocity. The pebble flux is,

$$\dot{M}_{pebb} = 2\pi r_g \frac{dr_g}{dt}(Z\Sigma_g), \tag{1.10}$$

and Z is the fraction of solids to gas that can be used to produce pebbles. Pebbles are produced at the pebble production front r_g that evolves with time as

$$r_g = \left(\frac{3}{16}\right)^{1/3} (GM_{star})^{1/3}(\epsilon_D Z)^{2/3} t^{2/3}, \tag{1.11}$$

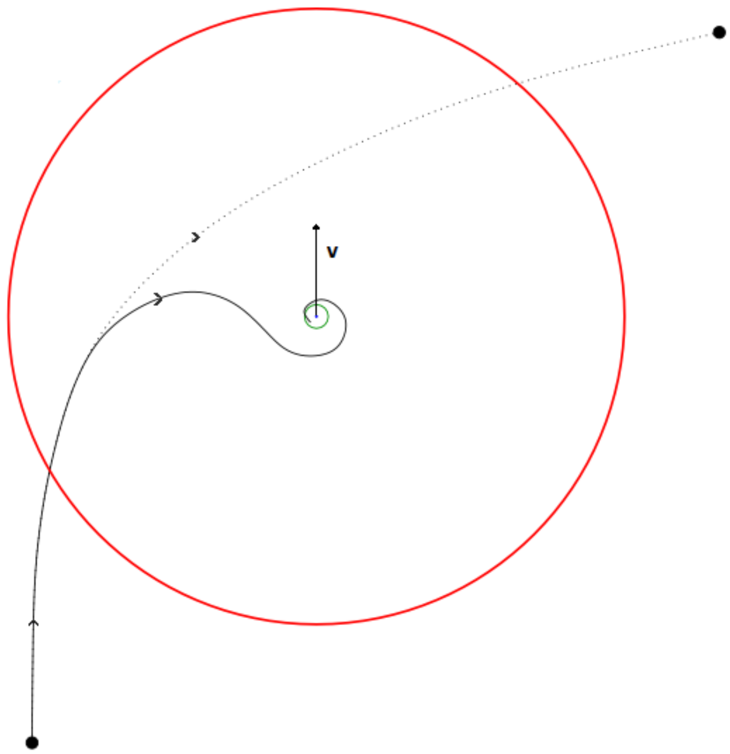

Figure 1.5: Illustration of a pebble (solid line) spiraling in towards a protoplanet. With a protoplanet in the centre, the green circle is the gravitational cross section, the red circle is the hill radii. The dotted line represents a planetesimal that are decoupled from the gas and are scattered away, even when entering the hill sphere.

$$\frac{dr_g}{dt} = \frac{2}{3}\left(\frac{3}{16}\right)^{1/3}(GM_{star})^{1/3}(\epsilon_D Z)^{2/3}t^{-1/3}, \tag{1.12}$$

where the parameters $\epsilon_p = 0.5$ and $\epsilon_D = 0.05$, they are free parameters that can be used to regulate the coagulation efficiency of dust into pebbles (Lambrechts & Johansen 2014). This tell us that the pebble accretion rate scale with the planet mass, as the mass increases the planets hill radii. We can also see that the pebble production front is moving out with time, telling us that there is a pebble flux coming from the outer part of the disk where we want to grow the cores of the planets.

One important detail are that these equations assume a circular orbit. When planets interact they will excite each others orbits to some eccentricity. Eccentricity and inclination is damped by the gaseous protoplanetary disk, but not totally. Even an eccentricity of a few percent affects the relative velocity between the planet and the surrounding material (mainly pebbles), making it harder to accrete them. From figure 1.5 we can understand that if a pebble comes in towards the hill sphere to fast it will just fly by before it can get affected by the planets gravity and spiral in. This is taken into account in the simulation with dampening terms for the eccentricity and adjustments to the accretion equations due to eccentricity (Johansen et al. 2015). For lower mass planets (in type-I migration) the dampening scales with the surface density in the protoplanetary disk. For massive planets (in type-II migration) the effect of dampening is less known, but it is approximated that the dampening timescale is proportional to the migration timescale, migration is discussed in section 1.4.

1.3.4 Planet growth

The planet cores will grow by accreting pebbles from their hill radii, as explained in section 1.3.3. To do this the planet seeds must first have reached a threshold mass to have a large enough hill radii. This is called the pebble transition mass as explained in section 1.2. This growth stage will continue until the planet reaches a mass enough to perturb the surrounding gas, causing regions around it to orbit super Keplerian. This results in a halt of the radial pebble flux through the protoplanetary disk towards the star and the planet stops growing from pebbles as there is no pebble flux towards the planet. This mass is called the pebble isolation mass and given by,

$$M_{Iso} = \left(\frac{H/r}{0.05}\right)^3 M_{Earth}. \tag{1.13}$$

This gives a range of masses from 15-70M_{Earth} for planets in the 20-150AU range, which is roughly the range where the planet seeds are in our simulations. In figure 1.6 I plot the isolation mass as a function of radius for a typical protoplanetary disk structure in the age (2.5×10^6 years) where we put in the planet seeds. The mass value also varies with the disk structure and age as it is a function of the aspect ratio (H/r) which decreases as the stellar luminosity drops (explained in section 2.1.1 and 2.1.2).

While the mass of the core is still higher than the mass of the gaseous envelope it will still be a violent atmosphere that gets hit by material. These collision with minor bodies and some pebbles prevent the envelope from cooling, if it can not cool, it can not contract. During this period the planet will migrate the fastest, as it is as massive as it can be to still be in Type-I migration, and the Type-I migration scale with the planet mass (explained in section 1.4). But the planet is still not massive enough to open a gap and enter Type-II migration. So this is a transition period before the gaseous envelope can contract efficiently. The gas accretion follows,

$$\dot{M}_{gas} = 0.00175 f^{-2} \left(\frac{\kappa_{env}}{1cm^2/g}\right)^{-1} \left(\frac{\rho_c}{5.5g/cm^3}\right)^{-1/6} \left(\frac{M_c}{M_E}\right)^{11/3} \left(\frac{M_{env}}{0.1M_E}\right)^{-1} \left(\frac{T}{81K}\right)^{-1/2} \frac{M_E}{Myr} \tag{1.14}$$

where κ_{env} is the opacity in the planet envelope and we use $\kappa_{env} = 0.05cm^2/g$, f is a fudge factor to change the accretion rate to match other numerical and analytic results and normally set to f=0.2 (Piso & Youdin 2014), ρ_c is the density of the core where we use $\rho_c = 5.5g/cm^3$ (the Earths mean density), M_c is the core mass in earth masses, M_{env} is the envelope mass in earth masses, M_{yr} is mega years and T the temperature in Kelvin. When the planets have reached the isolation mass, they will keep accreting gas and build an envelope. Equation 1.14 holds until the envelope mass gets higher than the core mass, then the planets atmosphere starts to cool and contract, leading to rapid gas accretion. This is the stage when the planet start to carve a gap in the protoplanetary disk, leading

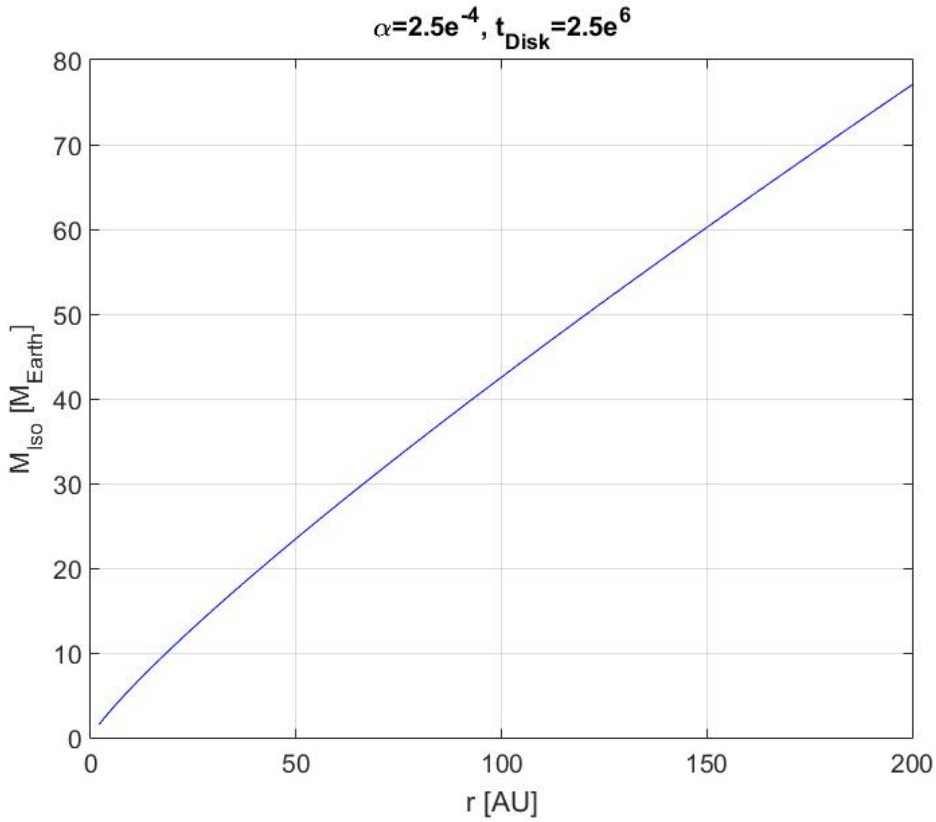

Figure 1.6: Pebble isolation mass as a function of radius for a 2.5×10^6 year old protoplanetary disk. Using an $\alpha = 2.5 \times 10^{-4}$.

to type-II migration, explained in section 1.4.2. The gas accretion in the runaway regime will then follow Machida et al. (2010),

$$\dot{M}_{gas,low} = 0.83\Omega_k\Sigma_g H^2 \left(\frac{r_{hill}}{H}\right)^{9/2} \qquad r_{hill}/H < 0.3, \tag{1.15}$$

$$\dot{M}_{gas,high} = 0.14\Omega_k\Sigma_g H^2 \qquad r_{hill}/H > 0.3, \tag{1.16}$$

where the minimum of $(\dot{M}_{gas,low}, \dot{M}_{gas,high})$ will be the active accretion. The “low” being for less massive planets where the core mass is still higher then the envelope mass, as we can see the term with the hill radii will grow with the planets mass and will dominate over the ”high” term, making the ”high” term the active one for higher mass planets. The maximum gas accretion rate is limited to 80% of the total mass flux through the disk (equation 2.2), as it is known that gas can pass the gap (Lubow & D’Angelo 2006).

1.4 Planet migration

When planets form in a protoplanetary disk they are affected by the gaseous environment they are in, and as the planets grow they will in turn affect the gaseous disk. These effects will cause the planet to migrate through the disk over the course of the disk lifetime. There are two main processes of migration - type I and type II as described below.

1.4.1 Type I migration

Around planets embedded in a gaseous disk there will be a gravitational gradient affecting the surrounding gas - causing a density wake that spirals radially in and out from the planet, due to the different orbit velocity inside (faster) and outside (slower). These overdensities in the disk exerts a force on the planets that results in a torque, a positive torque results in a increase in orbital radius. The outer wake exerts a negative torque and the inner wake exerts and positive torque. The sum of these are the wake torque, also known as the Lindblad torque. These wakes are illustrated in the left picture in figure 1.7.
The second torque to take in to account is the corotation torque. The gas that is in the same orbit as the planet will form into a horseshoe orbit, meaning that seen from the planets reference frame the orbit of the gas in this region looks like a horseshoe with the gap where the planet is, illustrated in the right picture in figure1.7.
Generally the Lindblad torque gives a negative torque and the corotation torque a positive torque, the sum of these are the resulting torque that cause the planet to migrate. The resulting torque is generally negative and depend on the disk properties where the planet is and strongly on the mass of the planet. The Lindblad torque scales as

$$\Gamma_0 = \left(\frac{M_p}{M_* h}\right)^2 \Sigma_p r_p^4 \Omega_p^2 \tag{1.17}$$

where h is the aspect ratio (H/r), Σ is the gas surface density and the index p indicates that we evaluate the quantities as the planets position.
Only taking the Lindblad torque into consideration (as it is the dominant torque), the timescale for a Earth mass planet to migrate into the star (under the simplification that the protoplanetary disk extends all the way to the star) from 1AU in the minimum mass solar nebula (MMSN) is about 300 000 years, which is a very short time in the lifetime of the protoplanetary disk.
But as we observe planets, both in and outside of our solar system they can not all migrate away. There are other migration processes that slow down the migration for massive planets. The corotation torque is one, and giant planets will move to type-II migration, described in section 1.4.2.

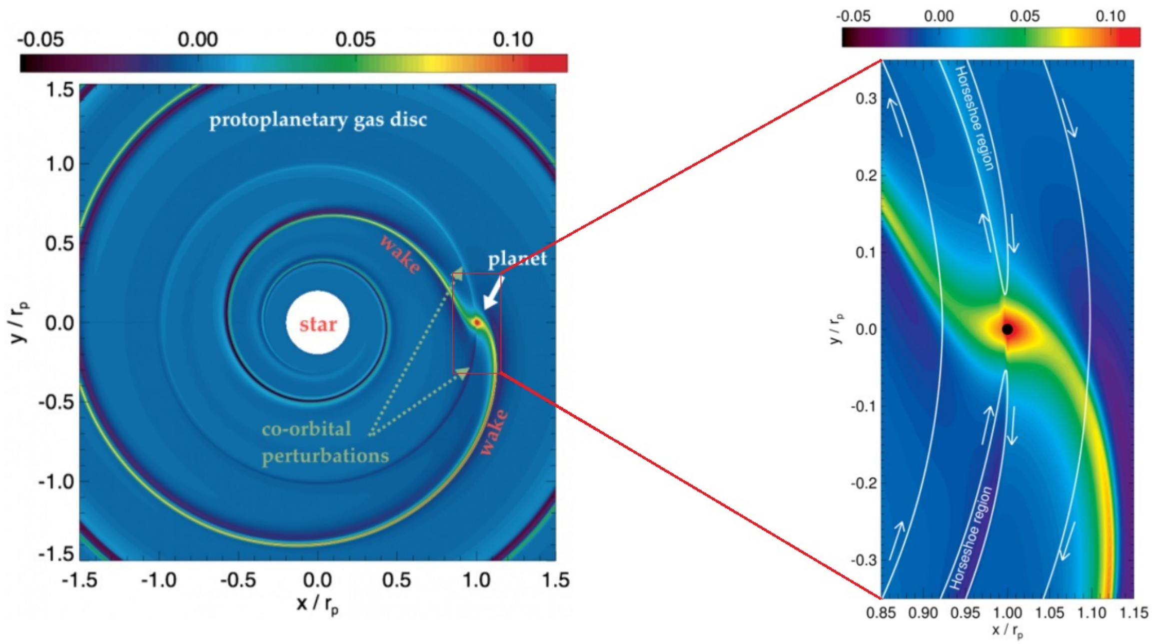

Figure 1.7: Left: Relative perturbation of the surface density of a gaseous protoplanetary disk perturbed by a 5 Earth-mass planet located at x=r_p and y=0. The planet induces a one-armed spiral density wave – the wake – that propagates throughout the disk, and density perturbations confined in the planet horseshoe region. Right: Zoom in to show the corotation/horseshoe region. Typical gas trajectories relative to the planet are shown with white curves and arrows (Baruteau et al. 2014).

1.4.2 Type II migration

When a planet is growing more massive (reach pebble isolation mass and envelope gets more massive then the core) it starts to perturb the gas around it more and more. If the planet is massive enough (also depending on the local properties of the disk) it will open a gap in the gaseous disk. When this happens the planet will no longer feel any torque from the gas (type-I migration) but will instead migrate with the viscous flow of the disk, that is much slower than the Type-I migration time scale.
As the planet grows it will exert a torque on the surrounding gas, an example of this is plotted in 1.8. In the gas there will be a competition between pressure and viscosity, represented by a parameter P. A gap will open if (Crida et al. 2006)

$$P = \frac{h}{q^{1/3}} + \frac{50\alpha}{qh^2} \leq 1, \tag{1.18}$$

where q is the mass fraction M_p/M_*, h the aspect ratio and α a dimensionless scale constant for the viscosity. The viscosity ν is defined as,

$$\nu = \alpha H^2 \Omega_k. \tag{1.19}$$

This effect on the gas has been simulated multiple times. Figure 1.9 shows the result of placing a Jupiter sized planet in a 3D gaseous protoplanetary disk and running it for 100 orbits. We can see a clear gap opened in the gas as a result of the planets presence[1].

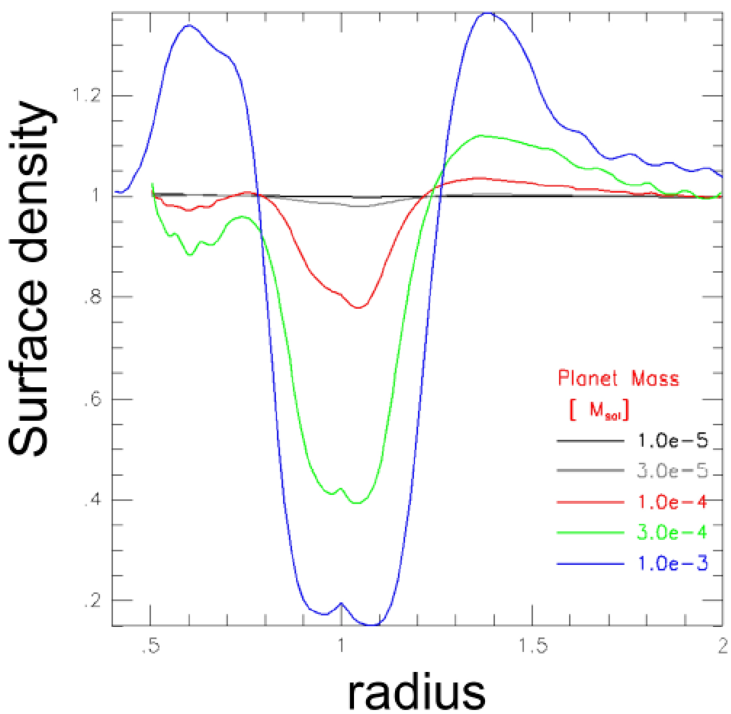

Figure 1.8: Showing the torque on the surrounding gas from the presence of a massive planet, normalized to the unperturbed gas. Where a value for the surface density>1 results in an acceleration the gas. Figure by: W.Kley

Using equation 1.18 and:

- h=0.05
- α=0.004
  $\Rightarrow$ gap if q> 10^{-3}

[1]Simulations by: Frédéric Masset (CEA), (http://fargo.in2p3.fr/)

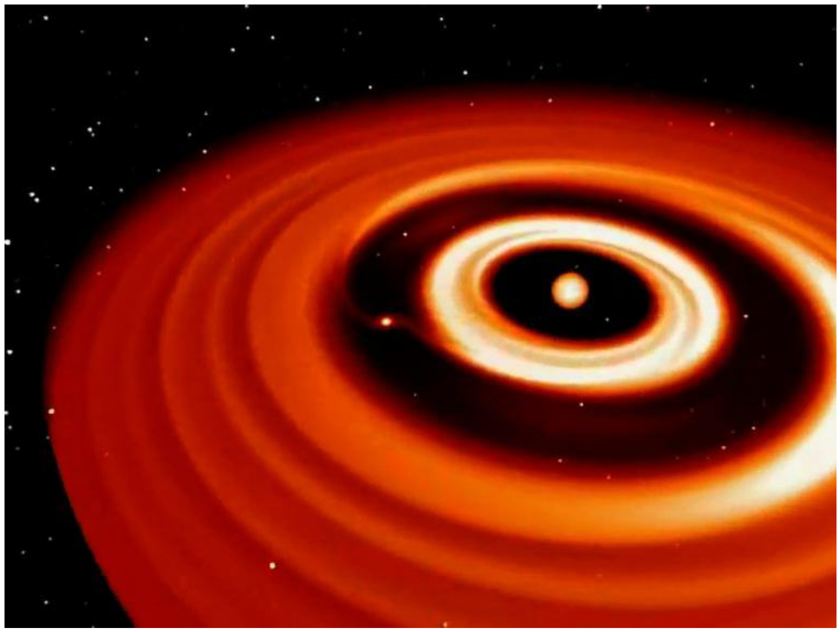

Figure 1.9: Snapshot after 100 orbits of a Jupiter inside a gaseous 3D protoplanetary disk. Simulation by: Frédéric Masset (CEA)

1.5 Previous work using pebble accretion

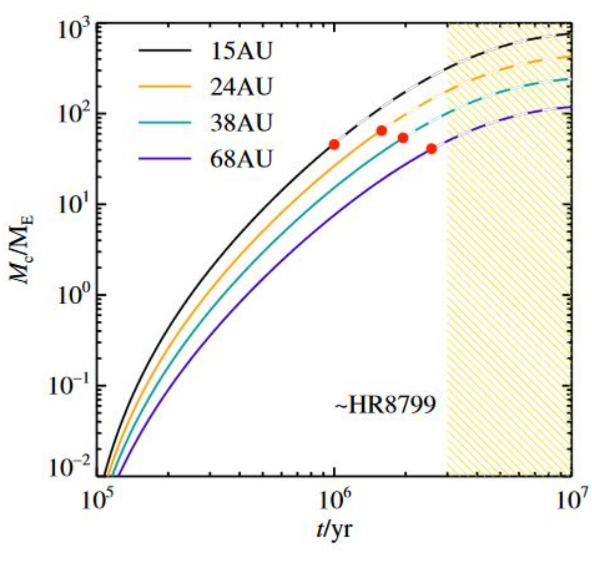

Figure 1.10: Growth curves for four planets seeds at different locations to grow the cores of the four giant planets in HR8799 using pebble accretion (Lambrechts & Johansen 2014).

As HR8799 is a well know system, prior work on the system exists. Lambrechts & Johansen (2014) were testing the pebble accretion model and successfully grew the cores of the planets in HR8799 as shown in 1.10. However, their aim was not to recreate HR8799 but to test the pebble accretion. In that sense they were successful, but as their aim was different than this project they did not include many mechanisms, such as migration, planet-planet interactions, gas accretion and a more accurate disk model corresponding to the system.
These simulations motivated our present study, which is to test the limitations of pebble accretion in a more realistic environment.

Chapter 2

Method

2.1 Disk structure

The first major step in this project is to create the structure of the disk that will serve as an environment for the planets to form in.

In Ida et al. (2016) they present a protoplanetary disk structure based on the temperature profile in the disk. This method makes sense because the aspect ratio and, with it, the density are directly linked to via hydro-static equilibrium,

$$T = \left(\frac{H}{r}\right)^2 \frac{GM_*}{r}\frac{\mu}{\Re}, \tag{2.1}$$

where μ is the mean molecular weight and $\Re$ the gas constant. Under the assumption of a steady accretion rate (not dependent on radius) we can then calculate the surface density from the relation,

$$\dot{M} = 3\pi\alpha H^2 \Sigma_g \Omega_k \tag{2.2}$$

where α is the viscosity parameter, H is the vertical scale height.
This is a good assumption, because if the accretion rate was not steady there would be build up of material and gaps would form, this would likely be nonphysical. Therefore if there are irregularities they are smaller then the mixing caused by viscosity. The accretion rate through the disk do evolve in time however, discussed in section 2.1.1.
In Ida et al. (2016) they suggest a two part temperature structure, depending on the dominant heating mechanism - viscus or stellar heating. Given by

$$T_{visc} = 200 M_{*0}^{3/10} \alpha_3^{-1/5} \dot{M}_{*8}^{2/5} \left(\frac{r}{1AU}\right)^{-9/10} K, \tag{2.3}$$

and,

$$T_{star} = 150 L_{*0}^{2/7} M_{*0}^{-1/7} \left(\frac{r}{1AU}\right)^{-3/7} K, \tag{2.4}$$

where we define,

$$M_{*0} \equiv \frac{M_*}{M_\odot},\ L_{*0} \equiv \frac{L_*}{L_\odot},\ \alpha_3 \equiv \frac{\alpha}{10^{-3}},\ \dot{M}_{*8} \equiv \frac{M_*}{10^{-8}M_\odot/yr}. \tag{2.5}$$

These two temperatures as a function of radius give us two power laws. Where at any point the temperature is T=max(T_{visc}, T_{star}), then as mentioned above the aspect ratio and the density are calculated from the temperature as a function of the radius, illustrated for a young protoplanetary disk (50k years) in figure 2.1.

In this project we also run several hydrodynamical simulation with Fargo3D[1], same code as used in Bitsch et al. (2015a) for the protoplanetary disk structures, for the hydro dynamics we used a grid with 772x92 cells, from 2-130AU. Integrated forward for 500 orbits (at 5.2AU) for the disk to reach a state close to equilibrium. Due to time constraints we could not make a disk with our hydro simulations for all ages, so we used the data we had to construct our own power law disk. Using the data for the aspect ratio, and with it the temperature in the disk, illustrated in figure 2.2, we could re-scale the Ida disk model for a better match.

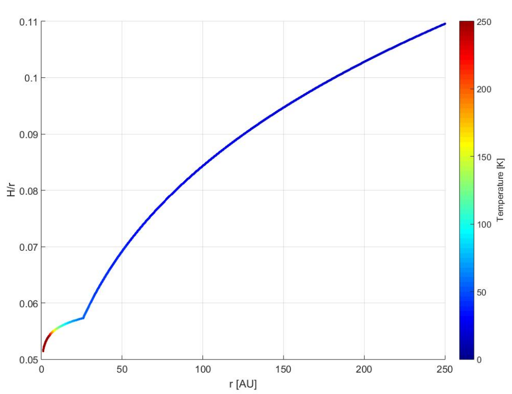

Figure 2.1: Aspect ratio as a function of the radius for the Ida disk structure. Color coded with the temperature.

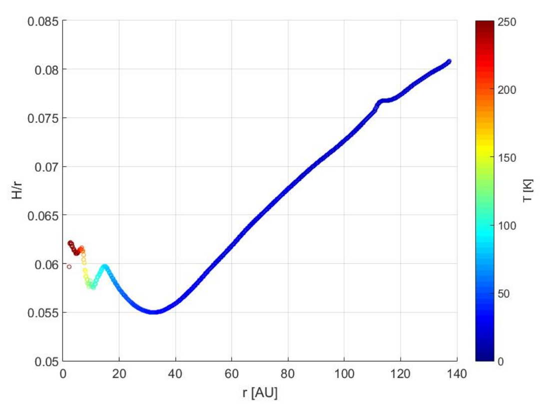

Figure 2.2: Aspect ratio as a function of the radius from Hydro dynamical simulations. Color coded with the temperature.

I set up my own power law disk, based on the equations in Ida et al. (2016), but scale the temperature equations to better match the results of my own hydro-dynamical simulation, all three plotted together for comparison in figure 2.3. One detail to note is that I focus on giant planet formation on wide orbits to re-create HR8799, meaning that

[1]FARGO3D was written by Pablo Benítez Llambay (main developper) and by Frédéric Masset. http://fargo.in2p3.fr/

a normally important part of the disk - the inner disk, is of little importance to us in this project. That is why the inner bump around 5-15 AU caused by the opacity transition of the (water)ice line is ignored. This works well for two reasons, the first being that the inner viscous dominated region goes away fairly fast(0.5-1 million years, shown in section 2.1.1), and we never put any planet seeds in the simulation before 2 million years. Second being that if planets migrate to far in they will not be similar enough to HR8799 to be considered a success. After the power law profile is calculated, the other parameters: core growth rate, pebble scale height/density are as in Lambrechts & Johansen (2014), explained in section 1.3.3. The gas accretion and migration is treated as in Bitsch et al. (2015b), explained in section 1.3.4 and 1.4 respectively.

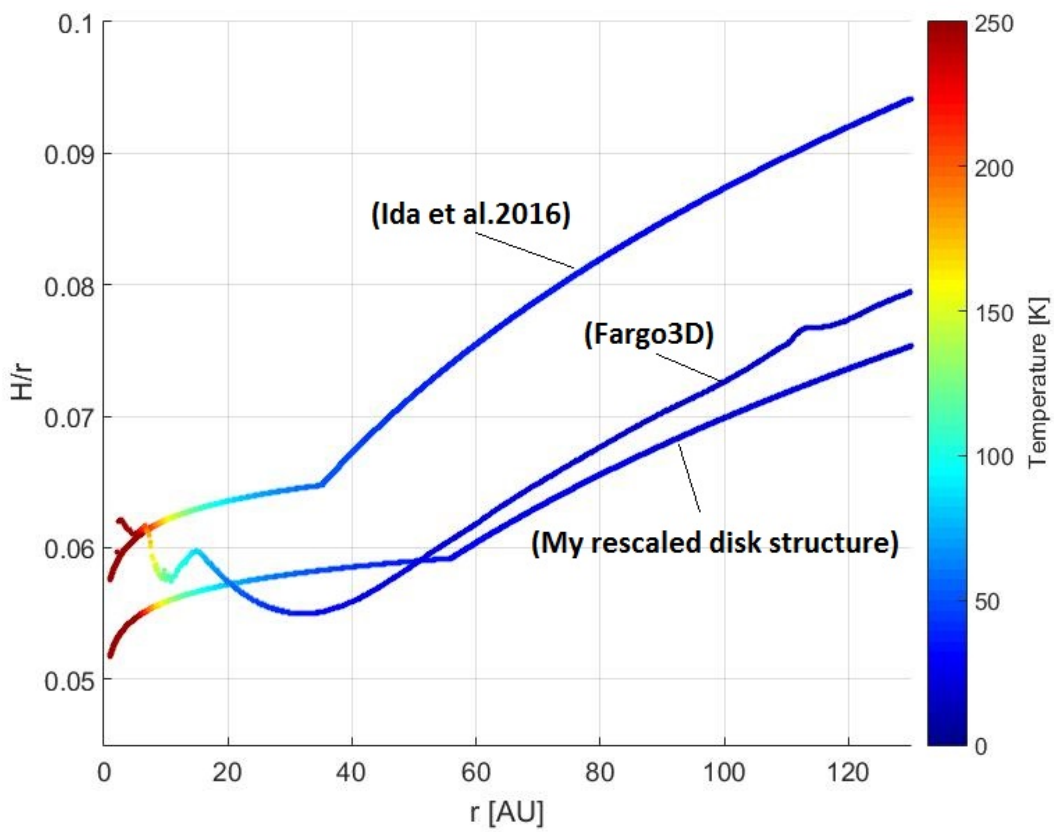

Figure 2.3: Showing my disk structure together with the original Ida disk structure and the result from one of our hydro dynamical simulations using Fargo3D, all for a 50k year old disk. Color coded with the temperature.

2.1.1 Disk evolution

A gaseous protoplanetary disk is not a static object, but a vivid evolving environment. From observations of stars with a protoplanetary disk we can see an excess emission in the UV, this emission corresponds to the accretion of material from the disk onto the star. The size of excess emission correlates to the mass accretion rate (Alcalá et al. 2014). With this we know how the accretion rate ($\dot{M}$) evolves in time for different stellar masses, plotted in figure 2.4. For a $1.5M_{\odot}$ star (used in this project) we follow the formula,

$$\log\left(\frac{\dot{M}}{M_{\odot}/yr}\right) = -7.69 - 1.4\log\left(\frac{t_{disk} + 10^5 yr}{10^6 yr}\right), \tag{2.6}$$

where t_{disk} is the age of the disk.

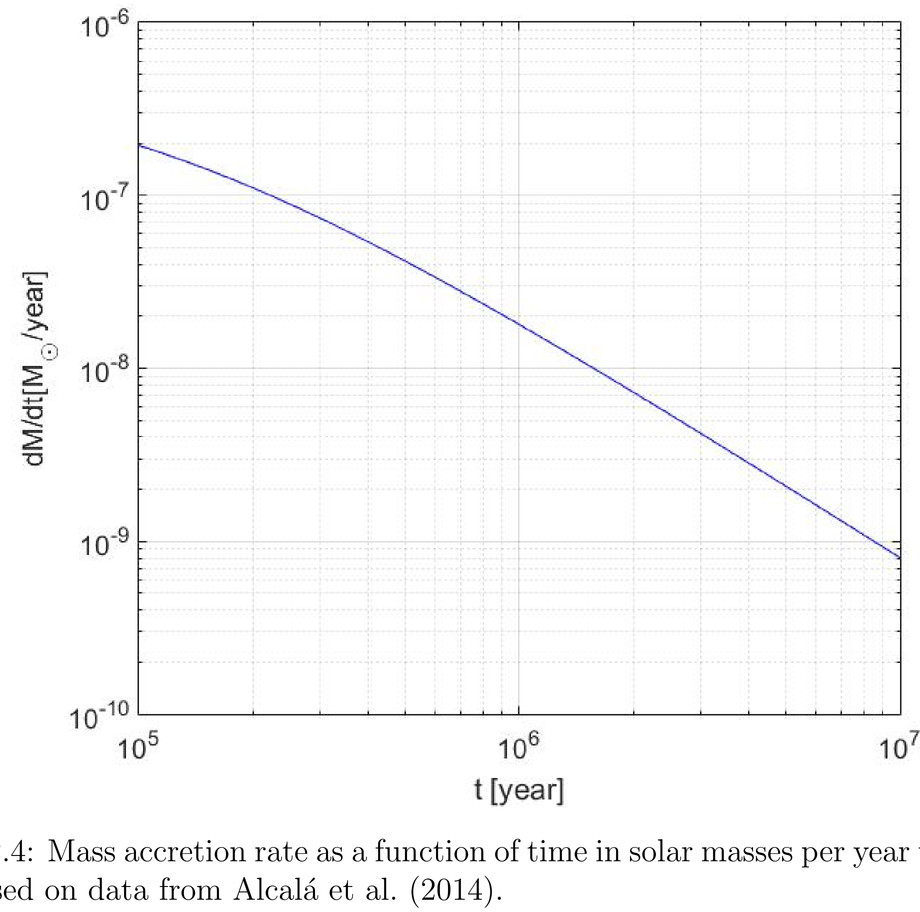

Figure 2.4: Mass accretion rate as a function of time in solar masses per year using equation 2.6. Based on data from Alcalá et al. (2014).

The change in the accretion rate combined with the luminosity evolution (discussed in section 2.1.2) translates into a change in the disk structure, that in turn will affect planets growth and migration. Figure 2.5 and 2.6 shows how the aspect ratio and the column density evolves with time in the protoplanetary disk structure used in this project.

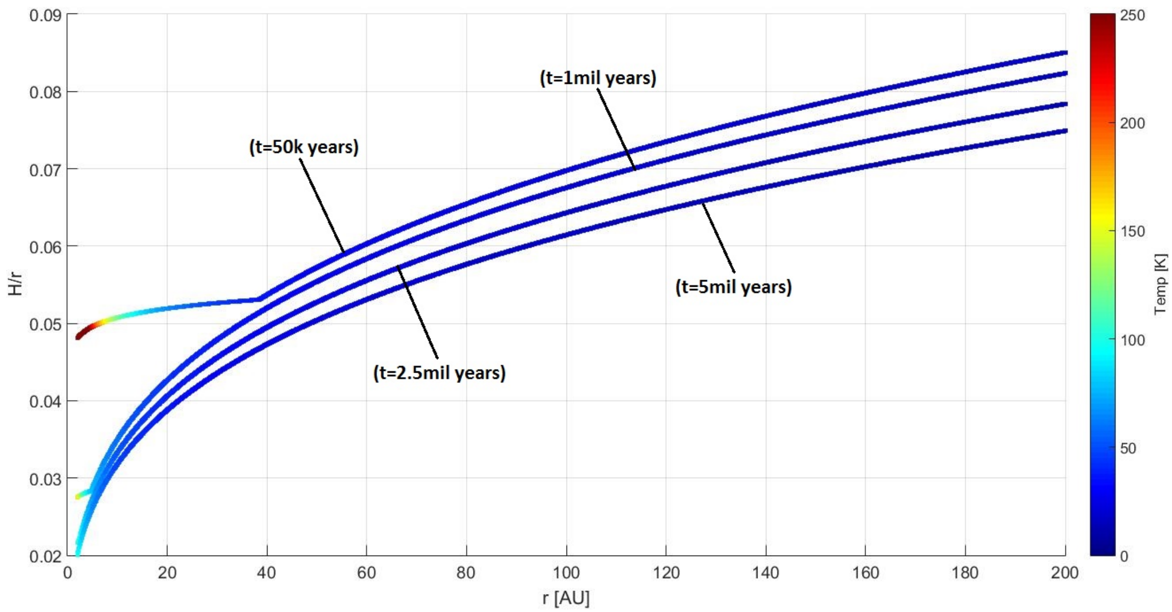

Figure 2.5: Showing how the aspect ratio evolves with time in the protoplanetary disk for the disk structure used in this project.

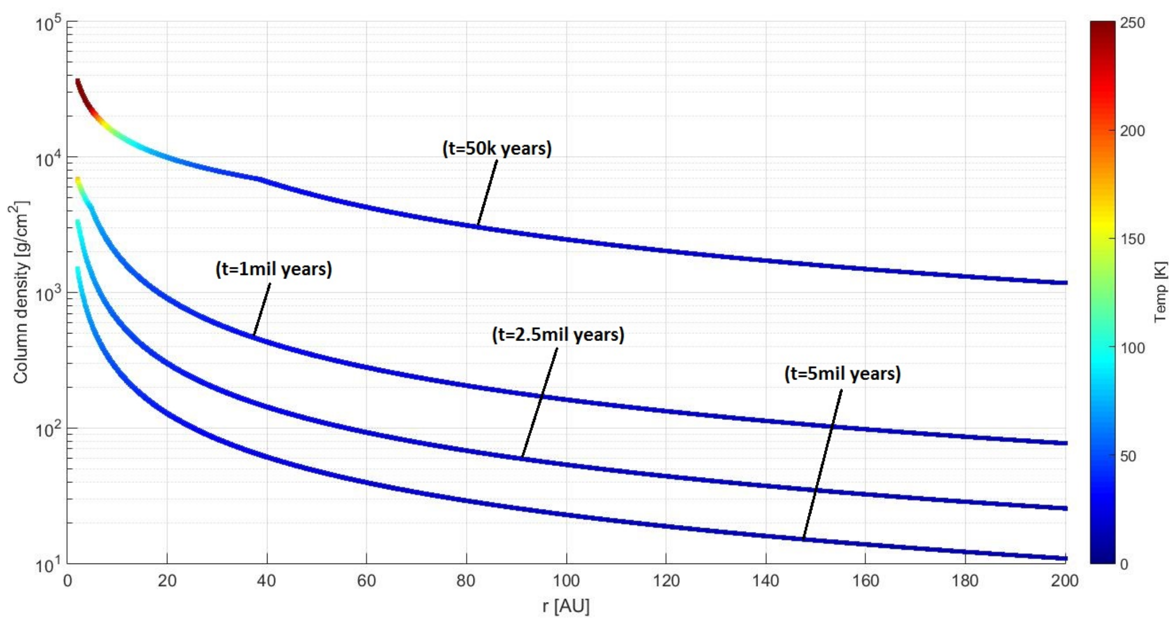

Figure 2.6: Showing how the column density evolves with time in the protoplanetary disk for the disk structure used in this project.

2.1.2 Stellar evolution

When a star is young it evolves rapidly, even in times scales comparable to the lifetime of protoplanetary disks, on the order of a few million years. This means that the changes in stellar properties need to be taken into account. The change that will be noticeable in this time is that the star contracts and heats up, so the radius decreases and the temperature increase. This change translates into a decrease in the stellar luminosity due to the reduced radii, that is an important factor in equation 2.4 for the temperature profile. That in turn translates into a change of the aspect ratio and accretion rates of material onto the planets. From stellar evolution models we can get the luminosity as a function of time, plotted in figure 2.7 (Baraffe et al. 1998). For our simulation we make a second order fit for the luminosity as a function of time, following

$$L(t) = [9.13778 \cdot 10^{-14} t^2 - 9.2614 \cdot 10^{-7} t + 3.9511][L_\odot], \tag{2.7}$$

where t is the disk age in years.

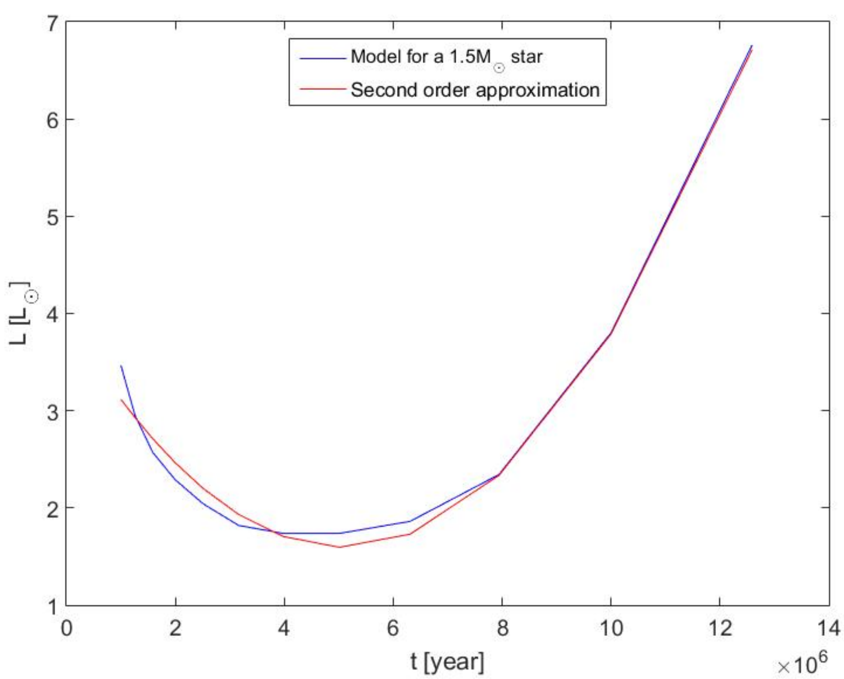

Figure 2.7: Stellar luminosity as a function of time with our second order fit over plotted.

2.2 Parameter probing

Before we can start the N-body simulation we need to probe and constrain the initial conditions. The main initial conditions used as input for the N-body simulations are the starting positions and time for the planet seeds. As the rate of which planets grow and migrate is very dependent on the turbulence and with it the density of where they are in the disk. The migration is also dependent on the mass of the planet as that affects how it interacts with the disk. I used an evolution code (Bitsch et al. 2015b) to make these kind of initial condition maps. To this code I implemented my disk structure (explained in section 2.1). In figures 2.8 and 2.9 we can see that one map gives us the initial time plotted vs the initial position of the planet seed, color coded to show the final planet mass, making every point on the map the result of one simulation. Overlapping in these maps we plot the lines at which planets end up at specific positions, in our case to match those of the planets in the HR8799 system (black lines), e.g 14.5, 24, 38 and 68 AU. In addition we plot the lower and upper limit of planet masses from observations (white and blue lines), e.g 4 to 9 Jupiter masses respectively. This tells us that we only need to focus on the area between the white and blue lines on the plot as any result over or under them will yield a to low mass planet, and over them too high mass planet. Now in this much narrower region we want to end up on the right positions as well, meaning we look at where the black lines are in this region.
These maps are then constructed for different α and pebble metallicity $Z = \Sigma_{pebb}/\Sigma_{gas}$. These are chosen as they greatly affect the disk structure, and in turn the planets growth and migration. Equation 2.2 showed us that if α is changed it translates into a change in the aspect ratio and/or the column density (as the $\dot{M}$ is constant). A change in the pebble metallicity directly affects the growth rate of the core via pebble accretion, as shown in section 1.3.3. With these maps we can see how the parameter space changes with different conditions and which input we can use for the N-body simulations. Figure 2.8 show the maps for initial time and position for planet seeds for $\alpha = 3 \times 10^{-4}$ and metallicity Z=0.015 in large scale for better viewing, figure 2.9 show the maps for the ranges of α used in this project, including two maps with lower metallicity to show how much harder it is to grow the planets with fewer solids.

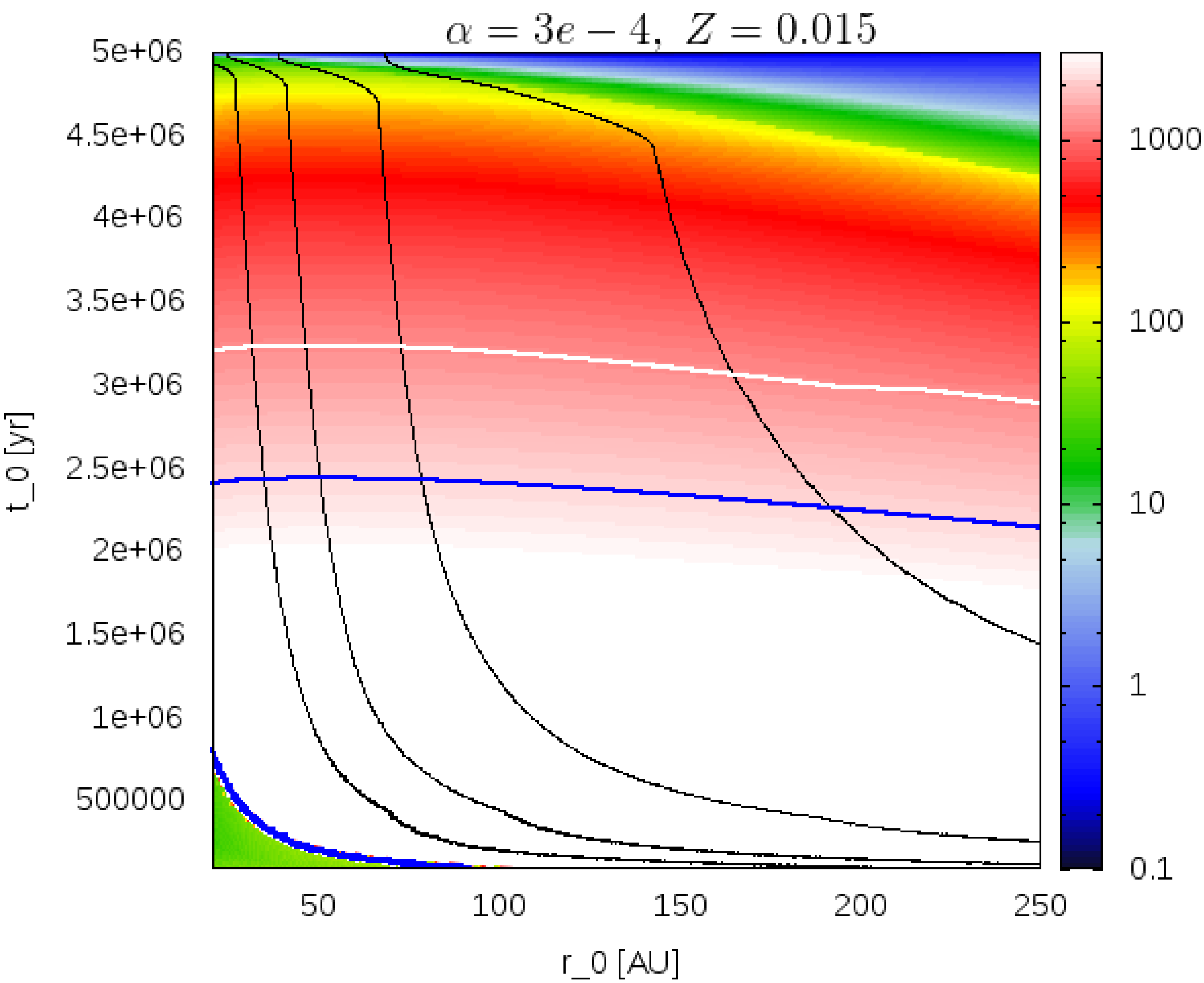

Figure 2.8: Maps for initial time and position for planet seeds for $\alpha = 3{\cdot}10^{-4}$ and metallicity Z=0.015. The color coding tells us the final mass of the planets. The white line is the $4M_{Jup}$ limit, everything under it being more massive. The blue line is the $9M_{Jup}$ limit, everything under it being more massive. So we want our planets to end in between these lines to match the observed planets in HR8799. The black lines are on which planets end up on the 14.5, 24, 38 and 68AU positions from the star, to match the final position of the planets in the HR8799 system.

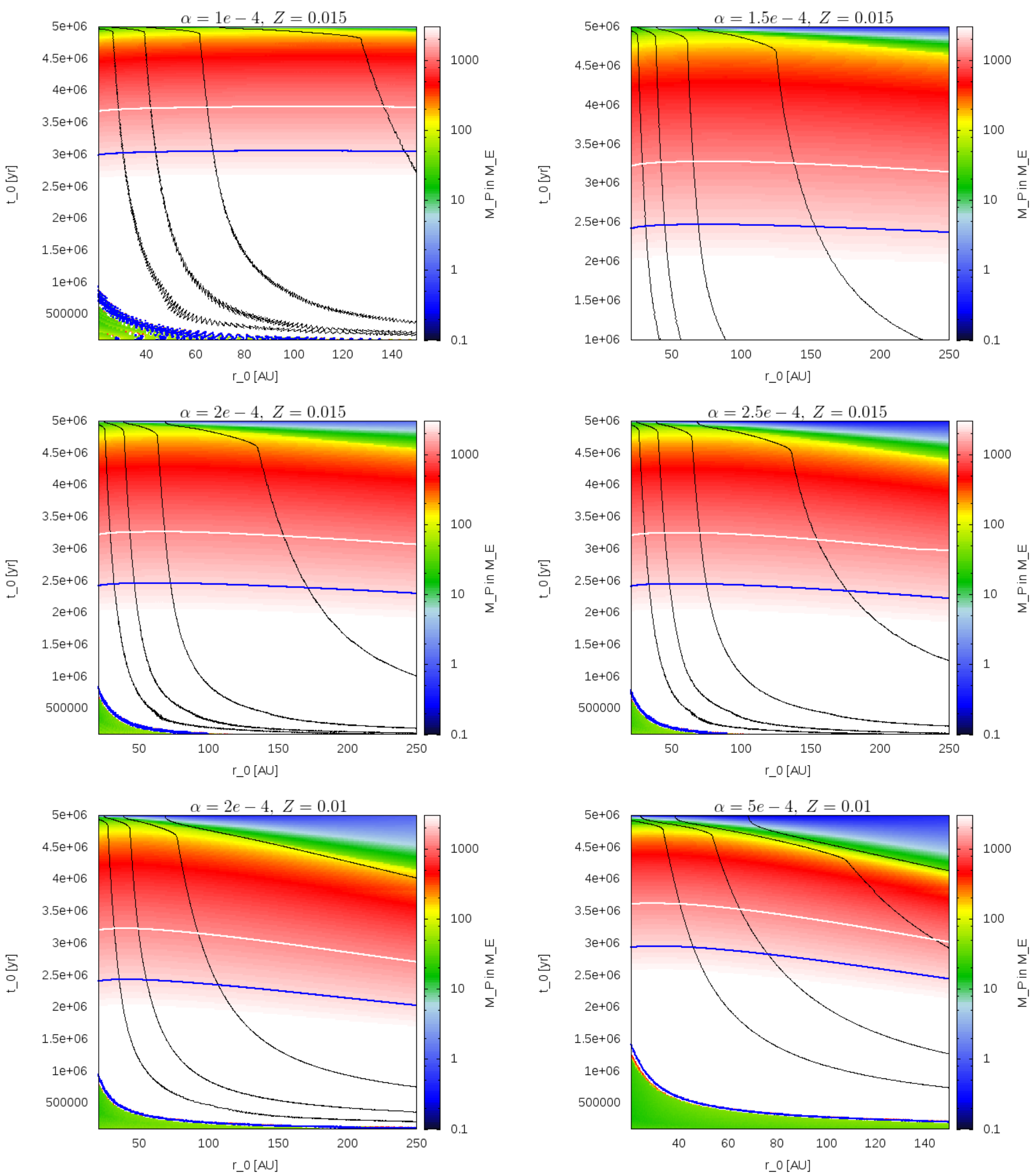

Figure 2.9: Maps for initial time and position for planet seeds. The difference in the plots is the viscosity parameter α and the pebble metallicity $Z = \Sigma_{pebb}/\Sigma_{gas}$ as noted over the plots. The color coding tells us the final mass of the planets. The white line is the $4M_{Jup}$ limit, everything under it being more massive. The blue line is the $9M_{Jup}$ limit, everything under it being more massive, as in figure 2.8.

2.3 Stability criteria

As we are exploring the possibility of forming the HR8799 system with pebble accretion we must make sure that the disk is not gravitational unstable. For a protoplanetary disk to be unstable it must satisfy both the Toomre (Toomre 1964) and Gammie (Gammie 2001) criteria. The Toomre criteria is about the mass in the disk,

$$Q = \frac{\Omega_k c_s}{\pi G \Sigma_g} = 1, \tag{2.8}$$

where c_s is the sound speed and the Q=1 sets the minimum mass for the disk to be unstable. Assuming a surface density proportional to 1/r, this can be re-written in good approximation as,

$$\frac{M_{disk}}{M_{star}} \approx 4\frac{H}{r}. \tag{2.9}$$

This is not true in our case, but is not far of and can still be used as an approximation and will give us an indication if the disk is getting massive enough to go unstable. For a 1.47 solar mass star it translates into,

$$M_{disk} \approx 6\frac{H}{r} M_{\odot}. \tag{2.10}$$

This is a full disk approximation to see if it contains enough mass to go unstable, if this is fulfilled we need to look closer at the radius dependent Q parameter, as gravitational instability is a local property.

By looking at the data from our simulation with the youngest disk, hence the most massive one as it has not got accreted to the star yet. So in the worst case scenario, I find that six times the H/r (aspect ratio) is in the range 0.32-0.5 in the outer part (the stellar heated region about 36 AU and out as seen in figure 2.5) of the disk where most of the mass is, hence the most likely region for instabilities. We have a disk mass that varies greatly with the input parameters. For the young disks (that are the most massive) we almost always fulfilling this criteria. But as we know, if any planets formed like this very early they likely migrate into the star very fast and are lost, so we look close at these criteria at different disk ages closer to the times where we need to start our planet seeds. This means that we must take the next step and find out if we satisfy the cooling criteria (Gammie) as well. For the disk to be unstable and collapse it must cool fast enough so clumping can occur. Cooling time is given by,

$$t_{cool} \approx \frac{c_p T \Sigma}{\sigma_{SB} T_{eff}^4}, \tag{2.11}$$

where c_p is the heat capacity. I use the heat capacity for hydrogen as the disk is dominated by hydrogen gas. T is the column temperature, Σ the column density, σ_{SB} is the Stefan-Boltzmann constant and T_{eff} is the surface temperature of the disk. Meaning that this is a ratio of current thermal energy over the rate at which it radiates away. For the Gammie criteria to be fulfilled the following inequality must be satisfied,

$$t_{cool} < \frac{3}{\Omega_k}. \tag{2.12}$$

When this is fulfilled it means that the disk cools faster the mixing or heating can take place. Meaning fast enough for it to clumps and form planets, given there is enough mass. To test the disk stability I made maps of the disk age as a function of the maximum outer edge of the disk and color coded it with the disk mass. I included both the criteria for disk instability and checked versus them for every radii, if they both would be fulfilled it would be color coded with pink to stand out, the maps are shown in figure 2.10.

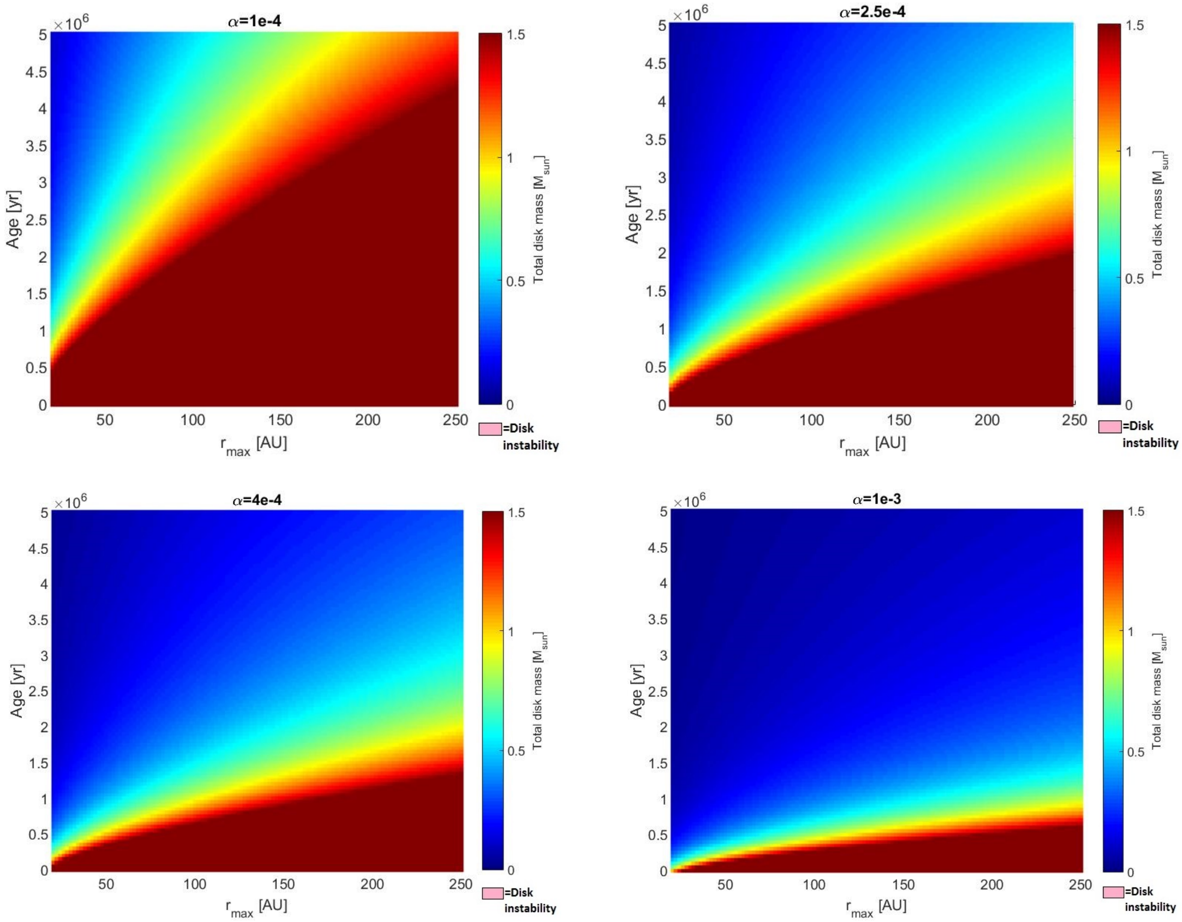

Figure 2.10: Maps of disk mass as a function of r_{max} integrated up to (disk size) and disk age. For different α values as indicated over the maps. Apart from the disk mass there is also a disk stability criteria color coded, in the case of an unstable disk there would be a pink dot. As we do not see any we know that we never satisfy both the Toomre and Gammie criteria, explained in section 2.3.

2.4 *N*-body simulations

We have our disk structure and our input parameters for the planet seeds. Now we must explore how the planets grow while interacting with each other. This will present multiple known problems, as well as reveal new unknown ones. There are two main known issues that will arise and make the planets deviate from their predicted growth tracks.
The first being that when the planet cores grow via pebble accretion they reduce the pebble flux through the disk, this can mean that the inner planets might receive less pebbles - hence making them grow slower than expected.
The second is that when planets interact they will make each other sightly eccentric. Eccentricity and inclination is dampened in the gaseous disk, but not totally. And even a small change in the eccentricity will cause a planet to orbit in a different velocity than Keplerian, this means that the relative velocity between the planet and the pebbles will change and it will be less likely for the planet to accrete the pebbles.
Based on the results from the parameter probing explained in section 2.2 we try to recreate HR8799 for different values of the α viscosity parameter and different starting ages of the protoplanetary disk and planet positions. To perturb the initial conditions for improving statistics we random the initial positions in the range [+1,-1]AU compared to the indication from the parameter probing.
So using a N-body code (modified version of the MERCURY code (Chambers 1999)) with an added parameterized space, corresponding to the protoplanetary disk. The disk structure is updated every 500 years in the simulation as the disk evolves in time as explained in section2.1.1 and section 2.1.2. So all interactions are taken into account, such as; planet-disk and planet-planet interactions, as well as planet growth via pebble and gas accretion, and planet migration.

Chapter 3

Results

3.1 Parameter probing

From our parameter probing we found an upper limit on α to be 5×10^{-4}. Even that is pushing it for it to be possible to form the outer planet in HR8799 as can be seen in the bottom right map in figure 2.9. As we know from equation 2.2, when we increase α the surface density goes down to compensate (as the accretion rate is constant). This makes it harder and harder to form the planets fast enough, meaning they have more time to undergo type I migration that is much faster than type-II. So to form the planets they must be initialized on wider orbits and earlier in the disk life time, and these parameters are limited by observations.
A lower limit on α is harder to determine. Initially we calculated a lower limit based on how massive the protoplanetary disk was - to satisfy the disk stability criteria discusses in 2.3. It is true that the lower we make α the more massive the disk becomes, but at the same time the cooling time goes up, keeping the disk stable. So the young and massive protoplanetary disks are a turbulent and vivid environment that are likely to be far from equilibrium, making it hard to apply the stability criteria on them in this state. A more realistic approach was to examine the stability in the disk closer to a disk age when the planets will start forming: $2 \times 10^6 - 3.5 \times 10^6$ years old. Even if the disk was unstable before that any planets formed would have migrated into the star on very short time scales of 10^4 years, meaning they would be lost long ago.

We find that according to the evolution maps we can make giant planets of wide orbits like those in HR8799. In figure 3.1 we see such a result, a $4M_{Jup}$ planet migrating in to 69AU at the time ($5{\times}10^6$ years) when the gaseous disk dissipates. The plot is also color coded with respect to time to show the direction the planets moves with time, as well as showing how much time is spent in the different stages of growth and migration.

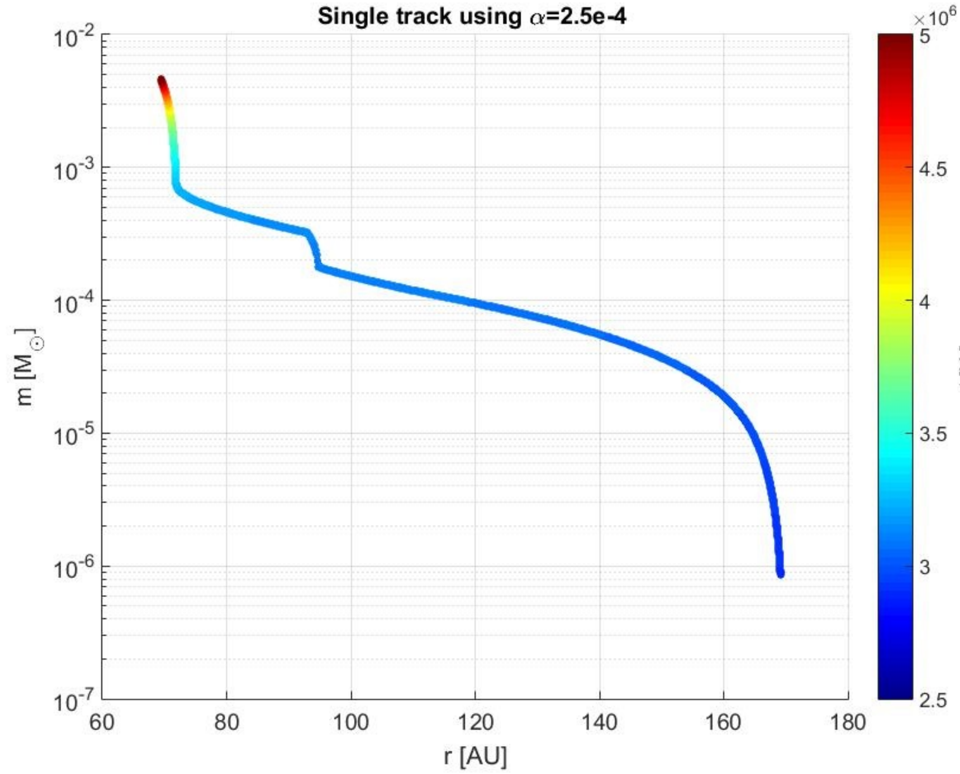

Figure 3.1: Single planet evolution simulation, showing that we can form giant planets at wide orbits. In this care a $\approx 4M_{Jup}$ planet is formed at 69AU. Color coded with time that show in which direction in the plot time flows and gives an idea how how long the different stages are.

3.2 Planet formation

When we simulate planets one by one we can find their expected growth curves and predict how large they will grow and where they will migrate as a function of the input parameters. Like initial position, α, disk age and pebble metallicity.

But when we have multiple planets they will reduce the pebble flux through the protoplanetary disk - as the outer planets accrete some of the material, there will be a reduced flux for the inner planets, making them grow slower than predicted.

And planets interact via gravity, meaning that the orbits of the planets will be perturbed by each other. Some effects of these interactions are known and expected, the question is how fast do they play a role and how big.
For the growth, the expected issue will come from the growing eccentricity of the planets due to interactions. The presence of the gaseous protoplanetary disk will dampen eccen-

tricity and inclination, but not totally. This means that the relative velocity between the planet and the pebbles will change and it will be less likely for the planet to accrete the pebbles, via the method described in section 1.3.3.
We found that initially most simulations start out with all four planets following their expected tracks. Until $0.4 - 1 \times 10^6$ years into the simulations, depending on planets sizes and growth rate, when most simulations go unstable. This results in planets ejected from the system or collisions. In figure 3.2 we see an example of such a run, where the expected tracks of the planets are included in the plot for comparison.

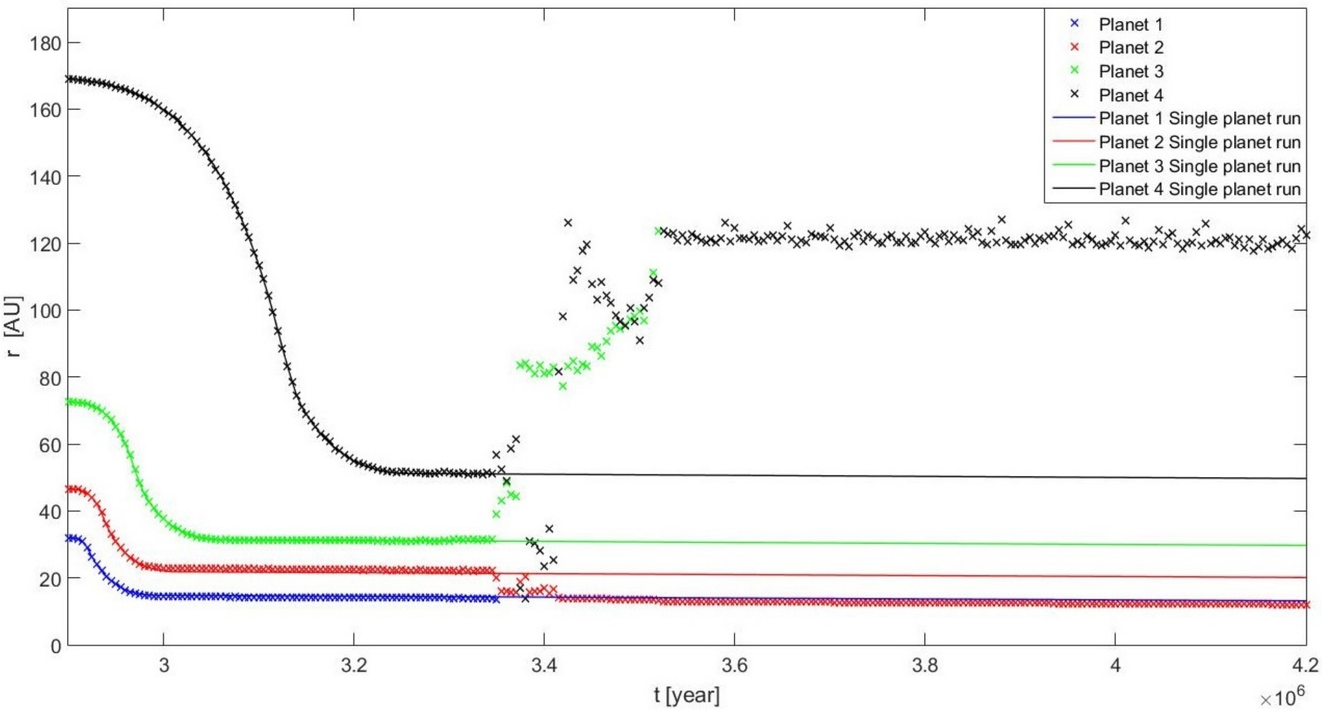

Figure 3.2: Comparing the result from one N-body simulation with four planets (marked with x) with the planets expected track if they where simulated one by one (the lines). This show us how much the planet-planet interaction disrupt each other, and even lead to ejection and collisions.

Since we are trying to recreate HR8799 it is bad for us that most of the simulations end with close encounters between the planets, making the system unstable. However, there are successful ones. A small percentage (8%) of the runs end up in a surviving system (up to the disk dissipation time of 5×10^6 years) with four giant planets on wide orbits. Out of these, three survive past the estimated age of HR8799 (39×10^6 years), up to 50×10^6 years. Not exact, but comparable to HR8799. As any system with multiple super Jovian planets on trans neptunian orbits are very rare, this result by itself is a success in showing that these type of systems can be formed via a core accretion scenario using pebble accretion. One example of a surviving system (run 50 in table 3.1) is plotted in figure 3.3. Showing

both the orbital distances and masses of the four planets. Resulting in three inner planets with about 3.8M$_{Jup}$ each, and the outer planet on 3.2M$_{Jup}$, the planets growth stops at the time when the gas in the protoplanetary disk dissipates as can be seen in figure 3.3. Ending up on orbits at 11, 18, 30 and 50AU, making them a bit closer in and less massive then the planets in HR8799, but a very comparable system.
As the estimated age of the HR8799 star is 30×10^6 years we also want to test the stability of the surviving systems up to and a bit beyond this time. This system was simulated up to 50×10^6 years showing no signs of instability, plotted in figure 3.4.

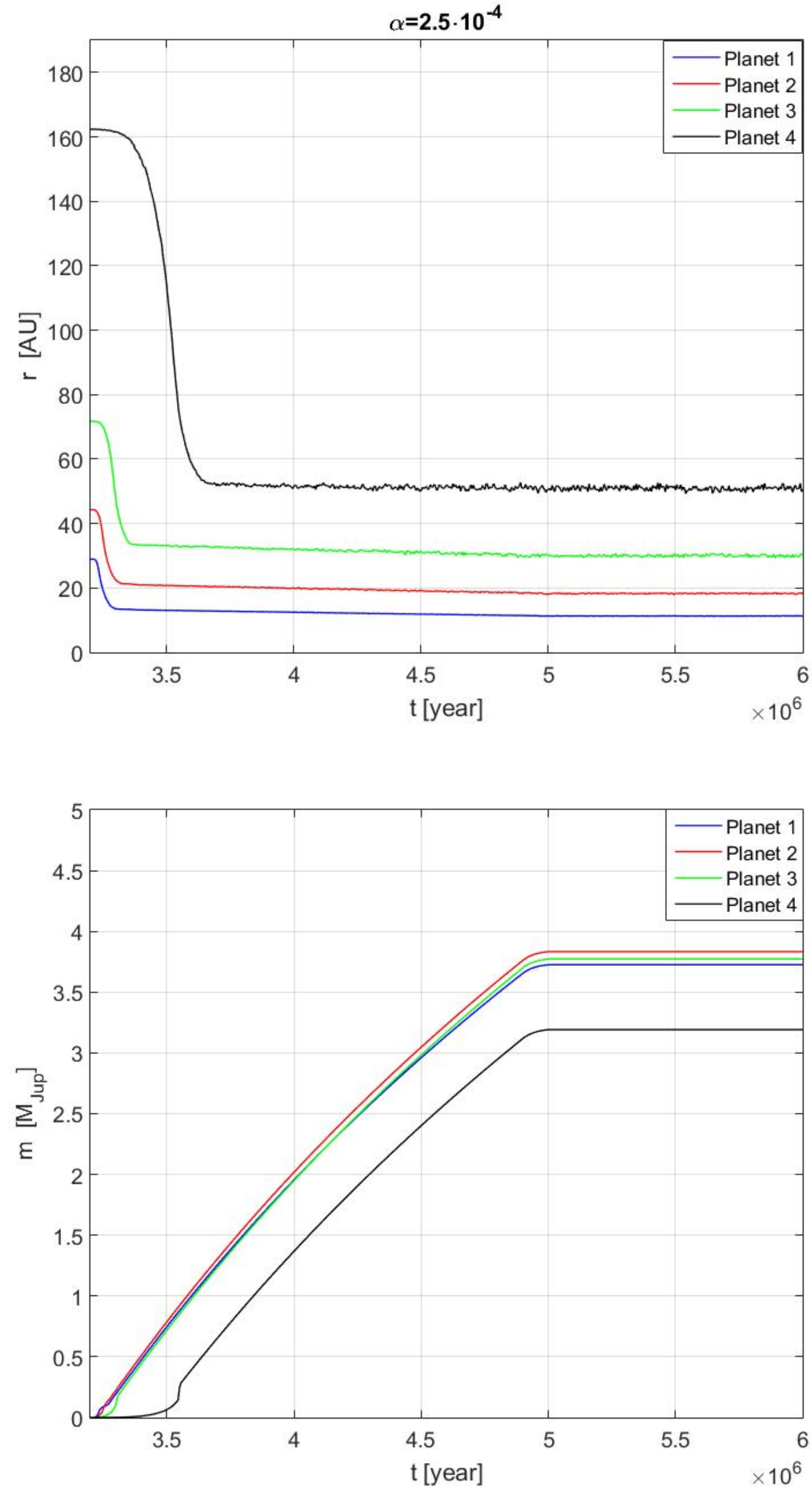

Figure 3.3: Result from one N-body simulation (run 50) up to $6{\times}10^6$ years, with a disk dissipation time at $5{\times}10^6$ years. Resulting in a HR8799 like system with four giant planets with wide orbits. Top plot showing their orbital distance as a function of time. Bottom plot showing the planet mass as a function of time.

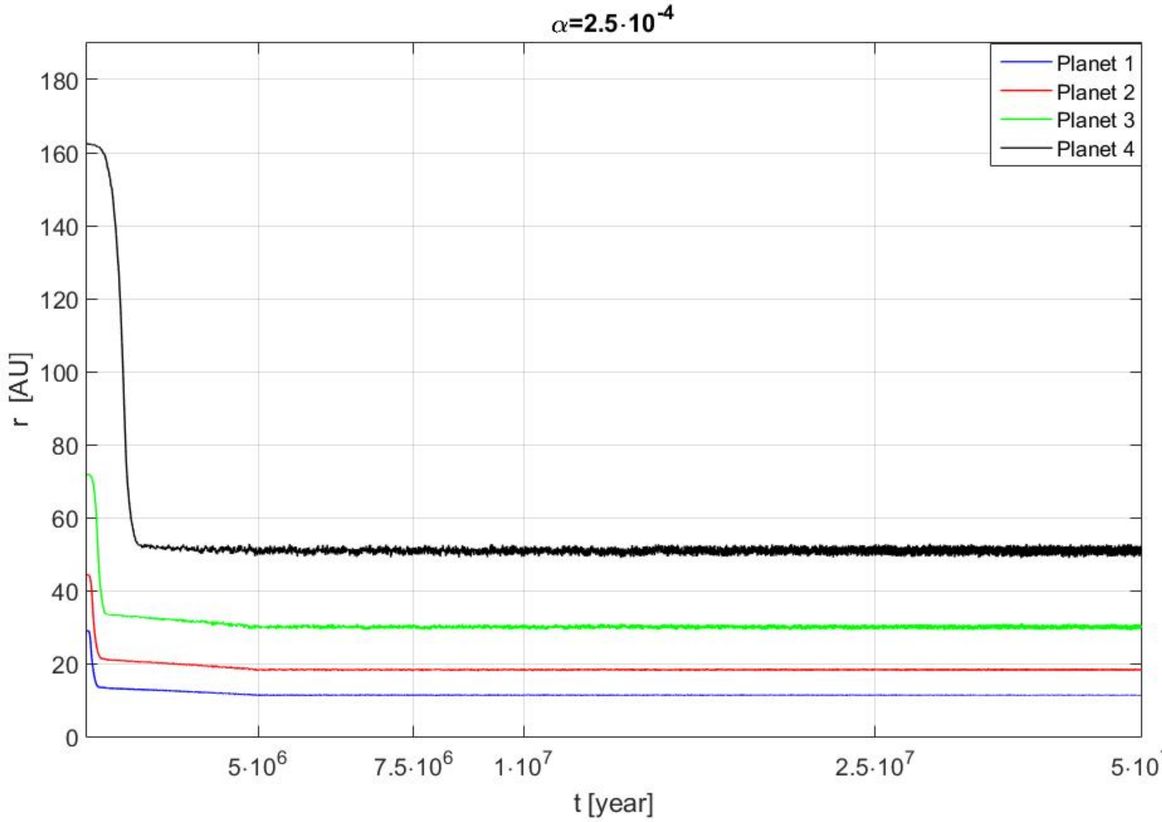

Figure 3.4: Result from one N-body simulation (run 50) on a longer timescale to test the stability of the system up to 50mil years, resulting in a stable HR8799 like system with four giant planets with wide orbits.

3.3 Simulations table and mean motion resonances

In this section I will provide a table of all full simulations, their run numbers corresponding to when I ran the simulation. So the "missing" numbers where various test simulation that are not included in this table.

The table also includes the calculated periods for the orbits of the planets just before interactions occurred. This was done to probe for possible mean motion resonances(MMR), and find out if there was a trend between the surviving simulations and the failed ones. MMR between two planets would mean that there is a even integer as a factor between their orbit times. For example while one planet makes one orbit around the star, the inner one makes two orbits, this means that stronger interactions repeat more regularly and often leads to instabilities. We found out that we do not see any clear correlation between the surviving systems and their MMR compared to the none surviving ones. Most of the runs have the two inner planets in or near a 2:1 MMR. Some runs also show the same relation between the two outer planets, and in some cases (such as run 32 shown in table 3.1) show very near 8:4:2:1 MMR with all four planets. But this is not as close for the other surviving systems and we have to little statistics to say for sure that the MMR is any indicator for stability, or viceversa.

Table 3.1: Table of simulations. Periods and masses are calculated just before the run goes unstable, for the surviving runs they are calculated after the disk dissipation time.
U = Unstable to early to determine.
Stable = stable up to 50×10^6 year.
End time is rounded to the closest 100k years. The error in the period is ± 0.5 years due to the fluctuations in the orbits.

Run	$\alpha[10^{-4}]$	Start t $[10^6]$	End t $[10^6]$	End m $[M_{Jup}]$	Periods [Yr]
29	2.5	3.2	29	3-3.8	36.76, 74.66, 151.83, 314.38
30	2.5	3.2	Stable	3.2-3.8	36.49, 74.15, 149.58, 308.74
31	2.5	3.2	0.7	1-1.7	40.1, 79.3, 144.6, 307.4
32	2.5	3.2	11.5	3.2-3.8	37.15, 75.66, 151.54, 306.78
33	2.5	3.2	7.5	3.2-3.8	34.9, 74.82, 150.9, 304.38
43	2.5	2.5	0.8	2.3-2.8	39.7, 80.2, 139.1, 302.2
44	2.5	2.5	0.4	1.8-2.3	45.3, 72.4, 146.1, 303.6
45	2.5	2.5	0.8	2.1-2.7	42.2, 77.7, 137.7, 302.3
46	2.5	2.5	0.2	0.2-1	U
47	2.5	2.5	0.7	1.8-2.2	43.1, 78.7, 138.2, 302.1
48	2.5	3.2	1.2	2.3-2.8	36.8, 75.9, 137.2, 300.5
49	2.5	3.2	0.6	1.1-1.7	41.4, 84.6, 143.6, 310.1
50	2.5	3.2	Stable	3.2-3.8	31.3, 64.4, 136.7, 301.1
51	2.5	3.2	0.8	1.4-2	40.2, 80.2, 140.6, 334.0
52	2.5	3.2	1.2	2.1-2.7	37.5, 76.5, 140.2, 303.6
53	2.5	2.5	0.4	1-1.3	45.5, 75.0, 151.4, 307.9
54	2.5	2.5	0.5	1.2-1.7	43.6, 77.4, 141.1, 300.2
55	2.5	2.5	0.2	U	U
56	2.5	2.5	0.5	1.2-1.8	41.8, 80.3, 141.4, 302.1
57	2.5	2.5	0.2	U	U
58	2.5	2.9	0.9	2-2.4	42.5, 74.3, 137.9, 301.4
59	2.5	2.9	1.1	2.7-3.2	36.9, 74.6, 135.9, 292.9
60	2.5	2.9	1.0	2.2-2.7	38.2, 77.6, 136.8, 298.4
61	2.5	2.9	0.8	1.8-2.2	38.7, 79.7, 139.4, 302.5
62	2.5	2.9	0.9	2-2.4	37.4, 77.8, 140.2, 298.2
63	2.5	2.9	0.9	2-2.4	38.0, 73.1, 139.6, 298.3
64	2.5	2.9	0.4	0.8-1.3	42.1, 86.4, 144.6, 304.4
65	2.5	2.9	0.6	1.2-1.7	41.1, 78.8, 147.5, 305.3
66	2.5	2.9	0.6	1.1-1.6	40.7, 84.9, 142.1, 305.8
67	2.5	2.9	0.8	1.7-2.3	39.2, 80.4, 143.4, 302.5
68	1.0	3.5	0.6	1.5-1.8	53.6, 88.9, 159.1, 322.0
69	1.0	3.5	0.6	1.5-1.6	51.9, 94.9, 156.7, 325.5

70	1.0	3.5	0.8	2.0-2.1	52.1, 93.0, 157.5, 324.0
71	1.0	3.5	0.7	1.7-1.8	49.5, 92.9, 152.8, 318.0
72	1.0	3.5	0.4	1.1-1.2	53.1, 90.2, 157.9, 322.3
73	1.0	3.5	0.9	2.0-2.1	52.8, 90.5, 152.6, 320.0
74	1.0	3.5	0.7	1.7-1.8	50.8, 91.8, 157.1, 324.8
75	1.0	3.5	0.5	1.2-1.3	52.3, 92.7, 155.1, 323.2
76	1.0	3.5	0.9	2.0-2.1	49.3, 92.0, 155.0, 323.7
77	1.0	3.5	0.8	1.6-1.7	55.1, 91.8, 154.9, 323.3
78	3.5	2.6	0.8	1.7-2.2	37.4, 77.2, 136.8, 294.2
79	3.5	2.6	0.8	1.5-2.5	38.2, 77.9, 140.8, 300.7
80	3.5	2.6	2.8	4.8-5.6	24.3, 58.5, 122.3, 282.4
81	3.5	2.6	0.5	0.5-1.3	U
82	3.5	2.6	0.8	1.5-2.5	36.6, 75.6, 139.8, 300.9
83	3.5	2.6	4.0	4.8-5.8	24.4, 55.7, 125.2, 268.4
84	3.5	2.6	0.3	U	U
85	3.5	2.6	1.0	2.0-3.1	35.3, 73.8, 135.5, 292.5
86	3.5	2.6	0.7	1.0-1.9	U
87	3.5	2.6	0.9	1.6-2.7	36.1, 76.5, 139.0, 295.2
88	3.0	2.7	0.9	2.0-2.8	36.4, 73.2, 137.5, 297.5
89	3.0	2.7	0.6	1.2-1.9	38.8, 79.3, 143.3, 304.0
90	3.0	2.7	0.6	1.0-1.8	40.8, 78.4, 142.9, 304.8
91	3.0	3.7	0.5	0.9-1.5	39.3, 79.6, 149.0, 305.9
92	3.0	2.7	0.9	1.9-2.5	37.2, 75.7, 139.3, 297.3
93	3.0	2.7	0.6	1.1-1.9	39.5, 79.7, 144.6, 305.4
94	3.0	2.7	0.7	1.2-2.0	39.3, 80.7, 141.8, 301.8
95	3.0	2.7	0.7	1.2-1.9	40.0, 81.2, 142.0, 300.7
96	3.0	2.7	0.6	1.1-1.8	40.2, 83.5, 142.8, 299.0
97	3.0	2.7	0.8	1.5-2.2	37.7, 78.0, 139.5, 297.8
98	2.0	2.9	0.6	1.3-1.6	45.0, 79.9, 145.2, 306.1
99	2.0	2.9	0.8	2.0-2.3	39.7, 81.5, 141.6, 306.3
100	2.0	2.9	0.4	0.8-1.1	U
101	2.0	2.9	0.9	2.3-2.7	38.6, 79.6, 143.3, 302.3
102	2.0	2.9	1.0	2.6-2.9	38.9, 79.5, 138.6, 303.1
103	2.0	2.9	0.7	1.8-2.1	44.8, 75.3, 143.2, 305.6
104	2.0	2.9	0.2	U	U
105	2.0	2.9	0.9	2.2-2.6	41.5, 76.4, 142.6, 303.5
106	2.0	2.9	1.1	2.6-2.9	38.1, 77.4, 140.0, 299.1
107	2.0	2.9	0.7	1.7-2.0	39.5, 80.1, 144.0, 307.5
108	1.0	3.0	0.9	2.1-2.2	44.4, 77.8, 143.7, 298.2
109	1.0	3.0	0.5	1.9-2.0	47.5, 81.2, 141.7, 301.1

110	1.0	3.0	0.7	1.7-1.9	46.2, 82.8, 147.8, 300.8
111	1.0	3.0	0.6	1.6-1.8	44.5, 82.5, 147.2, 300.1
112	1.0	3.0	1.1	2.7-2.9	44.4, 81.7, 140.2, 296.5
113	1.0	3.0	0.6	1.4-1.6	46.7, 79.3, 147.4, 300.2
114	1.0	3.0	0.5	1.3-1.5	47.0, 79.9, 147.3, 300.6
115	1.0	3.0	0.6	1.5-1.7	48.1, 82.4, 148.5, 308.1
116	1.0	3.0	0.8	2.0-2.2	47.0, 81.0, 143.5, 299.8
117	1.0	3.0	0.9	2.3-2.5	44.9, 81.5, 142.5, 293.5
118	3.0	3.0	29.5	3.6-4.4	29.4, 60.8, 133.1, 290.7
119	3.0	3.0	0.7	1.2-1.8	40.2, 76.7, 139.8, 302.4
120	3.0	3.0	1.1	2.0-2.8	35.8, 74.9, 140.2, 298.6
121	3.0	3.0	1.1	2.0-2.7	36.3, 75.6, 138.8, 298.2
122	3.0	3.0	0.4	U	U
123	3.0	3.0	1.0	1.8-2.5	37.2, 74.7, 137.7, 296.5
124	3.0	3.0	0.8	1.4-2.1	38.6, 75.6, 142.1, 302.6
125	3.0	3.0	2.2	3.7-4.5	31.4, 62.6, 130.3, 325.0
126	3.0	3.0	Stable	3.6-4.5	29.7, 60.1, 127.6, 293.8
127	3.0	3.0	7.2	3.6-4.5	29.6, 60.2, 127.9, 300.3
128	2.0	3.1	0.9	2.2-2.5	39.9, 79.5, 141.5, 306.0
129	2.0	3.1	0.7	1.6-1.9	39.9, 81.3, 149.2, 301.7
130	2.0	3.1	0.6	1.4-1.7	42.8, 78.6, 141.9, 308.0
131	2.0	3.1	0.6	1.3-1.6	39.1, 78.8, 147.5, 308.2
132	2.0	3.1	0.9	1.9-2.2	44.1, 79.9, 147.1, 308.9
133	2.0	3.1	1.1	2.6-2.9	38.2, 78.4, 141.2, 306,1
134	2.0	3.1	0.6	1.2-1.5	42.3, 85.6, 150.7, 305.5
135	2.0	3.1	0.2	U	U
136	2.0	3.1	1.2	2.6-2.9	38.1, 77.5, 140.8, 306.0
137	2.0	3.1	0.4	U	U

Chapter 4

Discussion

Since we are working in the field of exoplanet research, these results are but a piece of a larger puzzle. In this thesis we have explored the core accretion model using pebble accretion and shown that it is possible to grow giant planets on wide orbits. Our goal was to recreate a rare exoplanet systems with multiple massive planets on wide orbits, namely HR8799. While we do not find an exact match for HR8799 in our surviving systems we consider a big part of the project a success as we find surviving systems of comparable structure, with four giant planets on wide orbits. This tells us that is it likely that we could recreate HR8799 as well with further search in the parameter space.

With that said, we still only have a survival rate until the disk dissipation time (5×10^6 years) of 16.6%(5 of 30) for disks with $\alpha = 2.5 \times 10^{-4}$ and 15% (3 of 20) for disks with $\alpha = 3 \times 10^{-4}$. Out of these 8 survivors three (two for $\alpha = 2.5 \times 10^{-4}$ and one for $\alpha = 3 \times 10^{-4}$) were stable past the estimated age (30×10^6 years) of the HR8799 system, up to 50×10^6 years. All of the surviving systems are simulations with an old protoplanetary disk, meaning that the planet seeds are placed in the simulation at a later time. This is one of the reasons why the surviving systems have less massive (3.5-4.2M_{Jup}) planets than HR8799 (5-7M_{Jup}), as these planet seeds are plased in the disks at a later time, meaning that more of the meterial in the disk will have been accreted to the star, leaving the disk less dense, hence the cores grow slower. The slower growth also means that the planets stay in type-I migration longer, which is much faster then type-II, explaining why the planets migrate to closer orbits (10-50AU) compared to HR8799 (14-68AU).

As shown in this thesis and in previous work in Bitsch et al. (2015b), it is not hard to grow one planet almost anywhere in the disk. But when we have multiple planets, the dynamics play a major part - both for the planetary growth and the system stability. These low survival rates in our model are not surprising, as we observe very few systems with this type of configuration. This could be an effect of the majority of the systems that form with these configurations go unstable in astronomically speaking short timescales, on the order of 10^6 years. Another reason why we observe so few of these systems can also be more fundamental, that the timescale to grow the protoplanet seeds to the pebble transition mass to start rapid pebble accretion could be longer then we assume in this project. We place our seeds in after 2.5-3.5$\times 10^6$ years, while in reality it is not known on what timescales

the planet seeds grow.
We also believe that the survival rate is related to the migration rate of the planets when they enter type-II migration. The slower the planet grows in the early stage (higher α), the longer the planet stays in type-I migration, that is much faster than type-II, making it a more closely packed system, while a faster growth (lower α) does the opposite. But with a too fast growth we also observe a higher fraction of systems going unstable very early (under 0.5×10^6 years) due to the rapid type-I migration bringing the planets closer faster. With a faster growth the planets migrate faster in type-I migration, but for a shorter time, making the interactions between the planet grow very fast as they both grow in mass and get close to each other. So there seems to be a sweet spot in between for these type of systems. In figure 4.1 and 4.2 we can see the effect of only changing the α parameter. All five simulations have only one planet and same initial conditions apart from α. These plots show us that there is a clear difference in the growth and migration while in type-I migration. When they enter type-II migration their growth rate is the same, as it is capped (discussed in section 1.3.4). But there is a difference in the migration, as the planets reach type-II migration at different times and the type-II migration depends on the α coefficient. As we do not find any clear trend in the near mean motion resonances related to the surviving system we can not make any statement if it relates to the instability. Even among the surviving systems we have systems very near 1:2:4:8 resonance and others where only the two inner planets are close to a 1:2 resonance.
To test this hypothesis the next step in this project to recreate HR8799 would have been to take what we have learned and make small (realistic) adjustments to the protoplanetary disk structure. Such as making the temperature structure different and changing the disk lifetime. By varying the disk lifetime and the disk structure, which was not changed in this project, we could widen the search in the parameter space. Using what we learned in this project we have better constrains on α and know what factors to look out for (such as planet growth and migration speed). We could also vary the disk lifetime and temperature structure without having to redo all the work done in this project.

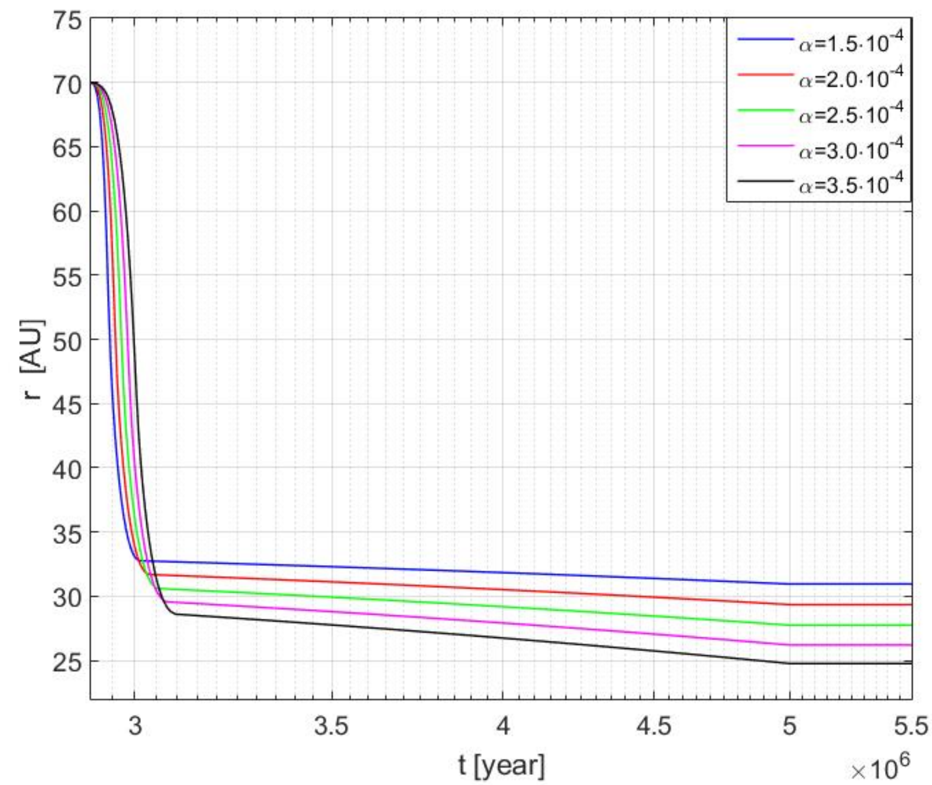

Figure 4.1: Aspect ration as a function of time for single planet simulations for different α. Show the difference in migration as a function of the viscosity. Where the rapid migration in the early part is type-I and the slower migration that follows is type-II.

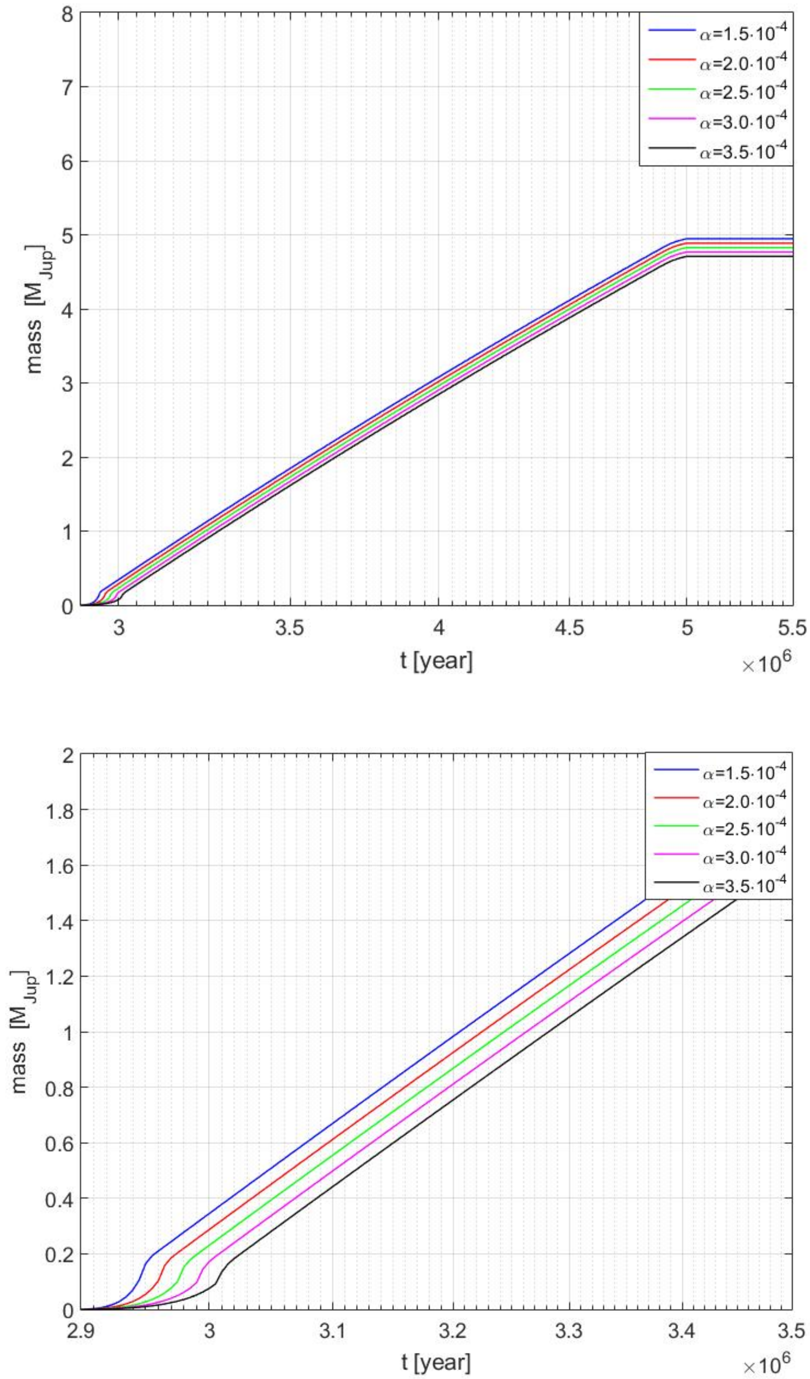

Figure 4.2: Top: Mass as a function of time for single planet simulations for different α. Bottom: Zoomed in to the early part of the simulation to illustrate the difference in the growth rate under the core growth phase.

Appendix A

Abundances

We are interested in the abundances of solids in terms of the percent of the total mass of the star, compared to solar. So I take the elements I have abundances for in HR8799: Carbon, Oxygen, Sulfur and Iron. Then I calculate the mass of these elements compared to solar and use their combined value as a metallicity in solids, as we care more about elements like Oxygen than Iron for the purpose of planet formation. So we rather want a general measurement of the abundance of solids and not just Iron.

Table A.1: Listing the percent of the Sun's mass by the elements used to approximate the solids in HR8799

Element	% of the Sun's mass
Carbon	0.40
Oxygen	0.97
Sulfur	0.04
Iron	0.14
Total	1.55

Table A.2: Measured abundances in HR8799 from Gray & Kaye (1999), Sadakane (2006) and Moya et al. (2010)

Element	Measured abundance	% change compared to solar
Carbon	[C/H]=0.1139	+30%
Oxygen	[O/H]=0.0414	+10%
Sulfur	[S/H]=-0.441	-64%
Iron	[Fe/H]=-0.470	-66%

Applying these percentage changes to the masses in the Sun yields,

$$Total_{HR8799} = 0.97\% * 1.1 + 0.4\% * 1.3 + 0.04\% * 0.36 + 0.14\% * 0.34 = 1.649\%. \quad \text{(A.1)}$$

So HR8799 have 1.649% of a solar mass in these solids. Divide the total for HR8799 with the total for the solar.

$$\frac{1.649\%}{1.55\%} = 1.06387 \tag{A.2}$$

$$\Rightarrow\ 1.06387 = 10^x \Rightarrow\ x = [Z/H] = 0.0269 \tag{A.3}$$

Where Z is the abundance in solids. Telling us that HR8799 is not so metal poor as it might seem if one would only look at the iron abundance.

Bibliography

Alcalá, J. M., Natta, A., Manara, C. F., et al. 2014, A&A, 561, A2

ALMA Partnership, Brogan, C. L., Pérez, L. M., et al. 2015, ApJ, 808, L3

Baraffe, I., Chabrier, G., Allard, F., & Hauschildt, P. H. 1998, A&A, 337, 403

Baruteau, C., Crida, A., Paardekooper, S.-J., et al. 2014, Protostars and Planets VI, 667

Baruteau, C., Meru, F., & Paardekooper, S.-J. 2011, MNRAS, 416, 1971

Bitsch, B., Johansen, A., Lambrechts, M., & Morbidelli, A. 2015a, A&A, 575, A28

Bitsch, B., Lambrechts, M., & Johansen, A. 2015b, A&A, 582, A112

Chainsson, E. & McMillan, S. 1999, Astronomy Today, 3rd Ed

Chambers, J. E. 1999, MNRAS, 304, 793

Crida, A., Morbidelli, A., & Masset, F. 2006, Icarus, 181, 587

Gammie, C. F. 2001, ApJ, 553, 174

Gray, R. O. & Kaye, A. B. 1999, AJ, 118, 2993

Haisch, Jr., K. E., Lada, E. A., & Lada, C. J. 2001, ApJ, 553, L153

Ida, S., Guillot, T., & Morbidelli, A. 2016, A&A, 591, A72

Johansen, A., Mac Low, M.-M., Lacerda, P., & Bizzarro, M. 2015, Science Advances, 1, 1500109

Lambrechts, M. & Johansen, A. 2012, A&A, 544, A32

Lambrechts, M. & Johansen, A. 2014, A&A, 572, A107

Lubow, S. H. & D'Angelo, G. 2006, ApJ, 641, 526

Machida, M. N., Inutsuka, S.-i., & Matsumoto, T. 2010, ApJ, 724, 1006

Mamajek, E. E. 2009, in American Institute of Physics Conference Series, Vol. 1158, American Institute of Physics Conference Series, ed. T. Usuda, M. Tamura, & M. Ishii, 3–10

Marois, C., Macintosh, B., Barman, T., et al. 2008, Science, 322, 1348

Marois, C., Zuckerman, B., Konopacky, Q. M., Macintosh, B., & Barman, T. 2010, Nature, 468, 1080

Moya, A., Amado, P. J., Barrado, D., et al. 2010, MNRAS, 406, 566

Piso, A.-M. A. & Youdin, A. N. 2014, ApJ, 786, 21

Sadakane, K. 2006, PASJ, 58, 1023

Toomre, A. 1964, ApJ, 139, 1217

Yang, C.-C., Johansen, A., & Schäfer, U. 2015, in AAS/Division for Extreme Solar Systems Abstracts, Vol. 3, AAS/Division for Extreme Solar Systems Abstracts, 115.13